ABSTRACT BOOK

ICPMAT 2024

BRNO, 30th SEPTEMBER—3rd OCTOBER

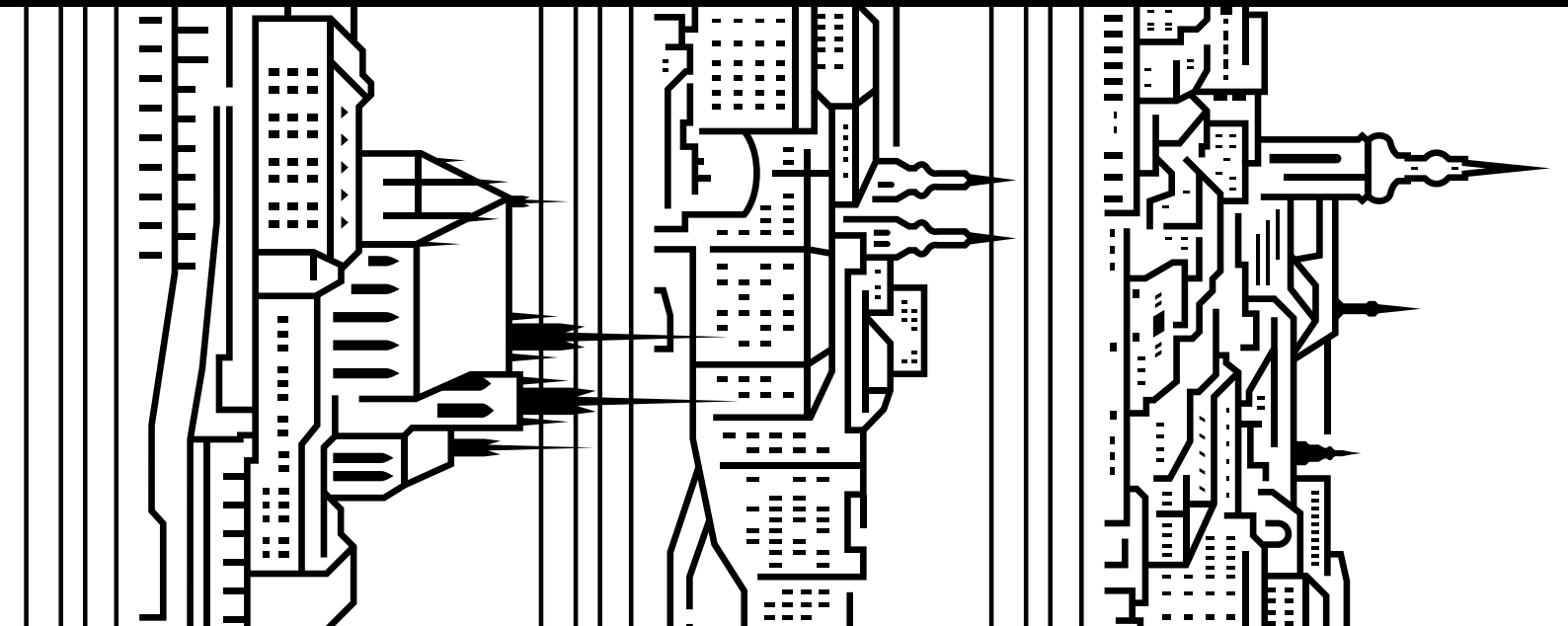

ABSTRACTS

Chapter IV 48–58

CHAPTER I

Application of FIB-SEM Serial-Sectioning Technique on Structural Materials

Toru HARA[1*], Hideaki NISHIKAWA[1], Takashi MICHIKAWA[2], Hideo YOKOTA[2]

[1]Research Center for Structural Materials, National Institute for Materials Science, Ibaraki, Japan.

[2]RIKEN Center for Advanced Photonics, RIKEN, Saitama, JAPAN.

**Corresponding author: HARA.Toru@nims.go.jp*

Three-dimensional(3D) microstructural analysis plays a vital role in materials research. We have studied about the FIB-SEM serial sectioning techniques for 3D analysis, especially for structural materials. Examples of the results will be presented:

The first example is the 3D analysis of M-A (Martensite-Austenite constituents) microstructure in steel. The orthogonal FIB-SEM, which has excellent resolution and contrast, was applied to reveal the details of the M-A morphology. In this observation, a new image analysis method was also constructed to combine with the section-based light microscope 3D observation with a wider observation range.

In the second example, a large volume 3D-EBSD observation was performed by PFIB-SEM to analyze the propagation behavior of small fatigue cracks. In this case, images from multiple detectors were acquired in a single slice and analyzed to obtain the desired information by combining them.

In both cases, the development of the hardware has enabled advantageous observations such as high resolution and large volume. However, at the same time, new analysis methods have also been developed to obtain the required information.

Al Induced Engineered Cluster Evolution of Ag for Approaching of Highly Transparent Flexible Thin Film Heaters

Guoqing ZHAO[1], Tao WANG[1], Wei CHU[1], Yi SUN[2], Eunwook JEONG[3], Jungheum YUN[3], Guanghui MIN[1, 2*]

[1]*Key Laboratory for Liquid-Solid Structural Evolution & Processing of Materials (Ministry of Education), School of Materials Science and Engineering, Shandong University, Jinan, China*

[2]*School of Physics and Materials Science, Changji University, Changji, China*

[3]*Extreme Materials Institute, Korea Institute of Materials Science, Changwon, Republic of Korea*

**Corresponding author: ghmin@sdu.edu.cn*

Improving of Ag wetting on oxide substrate is important to suppress the prevalent three-dimensional growth to deposit ultrathin continuous and smooth films for optoelectrical applications. The strategies of introduce heterogeneous metallic dopants and seed layers has been proved to be effective as wetting inducers, however it also criticized for the nonnegligible optoelectrical losses originated from the alien metals. This report presents the effects of Al-doping on Ag growth and provides a method by limiting Al additive to the initial Ag cluster stages to minimize optoelectrical losses. High-resolution electron microscopy, depth-profiling X-ray photoemission spectroscopy, and X-ray diffraction techniques are used to observe the morphological evolution, chemical and crystallographic features of Ag films to clarify the impact of Al on manipulation of Ag cluster. Further numerical investigations confirm the unconventional, thermodynamically driven migration of Al and its effect on Ag cluster evolution. Consequently, ultrathin Ag film based transparent electrode with low losses and superior heating performance are achieved.

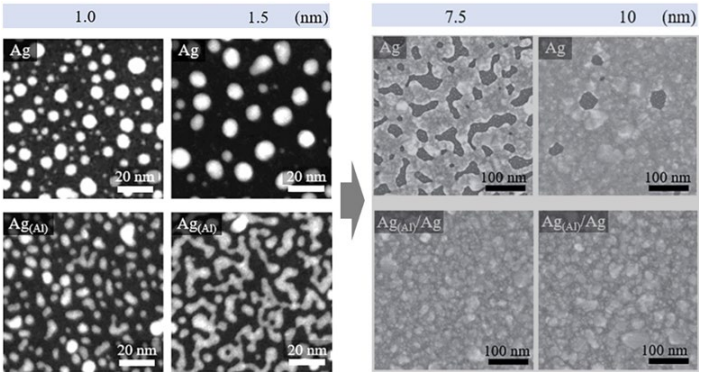

Figure 1. Morphological evolutions of Ag and Al-doped Ag ($Ag_{(Al)}$) clusters on SiO_x substrates (left) and 7.5, 10-nm-thick Ag films on SiO_x substrates with and without Ag(Al) wetting layer (right).

TEM observation of precipitates in Al-7%Si-0.3%Mg alloy

Taiki Tsuchiya[1], Seungwon Lee[1], Susumu Ikeno[2], Kenji Matsuda[1]

[1]Academic Assembly, Faculty of Sustainable Design, University of Toyama, Toyama city, Toyama, Japan

[2]Professor of Emeritus, University of Toyama, Toyama city, Toyama, Japan

**Corresponding author:: tsuchiya@sus.u-toyama.ac.jp*

Al-Si alloys have been used as casting materials for automobile parts. Al-Si-Mg alloys enhance its strength due to precipitation of metastable phase. Moreover, it is effective for increasing both strength and corrosion resistance with Mg addition. However, precipitation sequence is not clear in T5 condition. The aim of this work is to estimate mechanical properties and to clarify precipitates by Micro Vickers hardness measurement and microstructure observation of Al-Si-Mg alloy in T5 condition. Alloy was fabricated by casting using iron mold having Y-shape cavity. Alloy was cooled in the mold and temperature was measured. When temperature drops to 773K, alloy was quenched into ice water. After casting, artificial aging was carried out at 473K. Micro Vickers hardness measurement was performed using Mitutoyo HV-101 (load: 0.98N, duration time:15s). Microstructure observation were performed using Optical Microscopy (OM, OLYMPUS BX51M), Scanning Electron Microscopy (SEM, HITACHI S-3500H) and Transmission Electron Microscopy (TEM, TOPCON EM-002B). As the result of TEM observation in peak aged condition, There were needle-shaped precipitates along <100>Al direction and granular-shaped precipitates. The distribution of needle-shaped precipitates and granular-shaped precipitates were different from place to place. We analyzed needle-shaped precipitates and granular-shaped precipitates with HRTEM images.

TEM microstructure observation of Cu added excess Si-type Al-Mg-Si alloys

Seungwon Lee[1*], Shogo Asai[2], Taiki Tsuchiya[1], Kenji Matuda[1]

[1]*Graduate School of Science and Engineering, University of Toyama, Toyama, 930-8555, Japan*

[2]*Faculty of Sustainable Design, University of Toyama, Toyama, 930-8555, Japan*

[3]*Extreme Materials Institute, Korea Institute of Materials Science, Changwon, Republic of Korea.*

**Corresponding author: swlee@sus.u-toyama.ac.jp*

In this study, the precipitates behavior and mechanical properties according to aging treatment of ex.Si type Al-Mg-Si alloy with added copper were investigated. Figure 1 shows the precipitate abundance ratios according to the aging time aged at 473K. In the excess-Si alloy, at 0.48ks, which is the sub-aging stage, β‘‘ phase (parallelogram type) and random type precipitates were observed in a ratio of approximately 9:1. As aging continued, the amount of β‘‘ phase (parallelogram type) decreased and the amount of random type precipitates increased, and at 60ks the ratio was observed to be approximately 2:8. After that, when aging was continued up to 240ks, the amount of β‘‘ phase (parallelogram type) greatly decreased, and A-type, B-type, and C-type precipitates were observed. In the 1.0Cu-added alloy, as in the excess Si-type alloy, the amount of β‘‘ phase (parallelogram type) and random type precipitates were observed in the sub-aging stage, and when aging was continued up to the maximum hardness, the amount of β‘‘ phase (parallelogram type) increased and the amount of random type precipitates decreased. In addition, under these aging conditions, the pre-Q‘ phase began to be observed. When the aging time was extended to 60ks, the amount of β‘‘ phase (parallelogram type) greatly decreased, and the amount of pre-phase and Q‘ phase greatly increased. When aging was further advanced to 240 ks, the amount of pre-Q‘ phase decreased while the Q‘ phase continued to increase, and at 2400 ks only the Q‘ phase was observed.

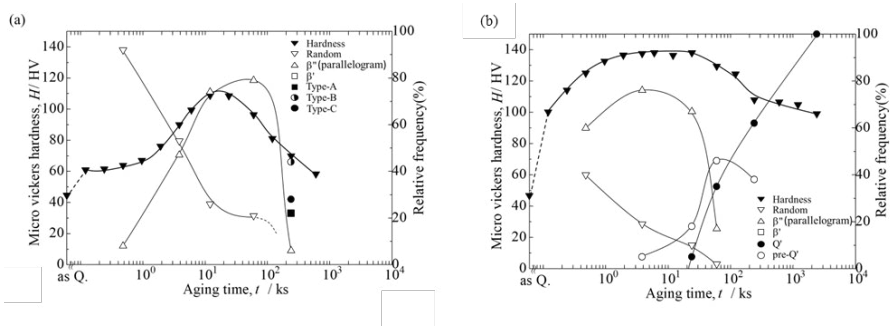

Figure 1. Fraction of precipitates of (**a**) ex. Si alloy, and (**b**) 1.0Cu added alloy

Understanding the Interplay of Microstructure Planar Defects for Improving the Mechanical Properties and Electric Conductivity Performance of Copper Foils

Artenis BENDO[1], Doriane Del FRARI[1], Adrian-Marie PHILIPPE[1], Patrick GRYSAN[1], Julien BARDON[1], Thomas DEVAHIF[2], Patrick CHOQUET[1], Nathalie VALLE[1*]

[1]Advanced Characterization of Surface, Interface, and Structure (ACSIS), Luxembourg Institute of Science and Technology (LIST), 41 rue de Brill, 4422 Belvaux, Luxembourg

[2]Research & Development Department, Circuit Foil Luxembourg (CFL), 9559 Wiltz, Luxembourg

**Corresponding author:: nathalie.valle@list.lu*

Abstract

The microstructure of electrodeposited copper foils containing two main planar interfaces – grain and twin boundaries – whose respective interfacial areas, densities and arrangements impact the mechanical properties and electrical conductivities of foils. Understanding the key microstructure planar interfaces and their effect on physical properties is crucial for precise control of foil microstructures and alternation of foil performance. With this aim, this work examines the microstructure of various copper foils produced through electrodeposition. Combination of advanced analytical methods allows to gain detailed insights from micrometer down to atomic-scale level. Energy-filtered transmission electron microscopy and focused ion beam scanning electron microscopy are used to characterize grain and twin structures. Mechanical properties and electrical conductivity are investigated using nano-indentation, tensile testing and four-point probe method, respectively. The relationships between the measured properties and grain/twin structures imaged on three planes, are correlated and importance of cross-section measurements is highlighted. The change on foil properties coincides with morphology transition of the grain shapes, sizes, and its consequence in the spacing of parallel twin interfaces.

Experimental procedure

Four distinct types of copper foils were electrodeposited at Circuit Foil Luxembourg (CFL) company into two thicknesses, 18 and 35 µm. The copper foils have two planar surfaces, i.e. the drum-side and the electrolyte-side surface, which correspond to the side electrodeposited onto the titanium drum and to the side facing the copper sulphate-based electrolyte, respectively. The grain structure imaging of planar surfaces was carried out by a dual-beam focused ion beam scanning electron microscopy (FIB-SEM). The cross-section microstructure imaging on the copper film thickness was done through the same procedure as planar surfaces but in this case, the freestanding copper foils were stuck up together and then transversally cut with a diamond

knife in an ultramicrotome, creating roughness-free surfaces. Transmission electron microscopy (TEM) was carried out on samples prepared either using focused ion beam or twinjet electropolishing. TEM samples were further thinned, and surface cleaned using a precision ion polishing system. Electrical conductivity was measured using the four-point probe method. Mechanical property characterization was done via nano -indentations and tensile tests. The atomic force microscopy (AFM) was employed to measure the surface topography and the nano-indentations marks on the copper film cross-sections.

Results

The relationship between these planar interfaces and foil performance is revealed through the correlation of microstructure parameters and measured elastic modulus, nano-hardness, tensile strength, ductility, and electrical conductivity.

A complete understanding of grain morphologies in the entire copper film thickness has been gained by studying the microstructure on three surfaces: drum-side, electrolyte-side, and cross-section. A critical grain size of around 0.6 µm is identified, for which there is a shape transition of grains from fine equiaxed to coarse elongated ones.

The grain size is observed to have a direct effect on twin interface spacing and therefore their density. Figure 1 shows that increase in grain size is positively correlated with increase in twin spacing that corresponds to the distance between the two coherent and parallel twin interfaces.

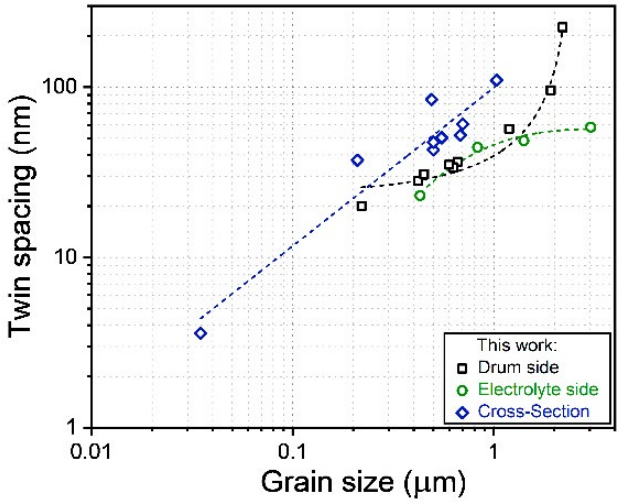

Figure 1. Relationship between twin spacing and grain size for planar surfaces (drum-side and electrolyte-side) and cross-section.

The grain size and the twin spacing are relative indications of the interfacial area of grain and twin boundary, which are present in the microstructure. The effect of grain size on conductivity and mechanical property is investigated. Figure 2 shows electrical conductivity dependence on grain size. The decrease in grain size in 500 – 50 nm range, is associated with a significant decrease in the conductivity. However, the twin interfacial area should be considered as well because the grain size influences the twin density (Figure 1).

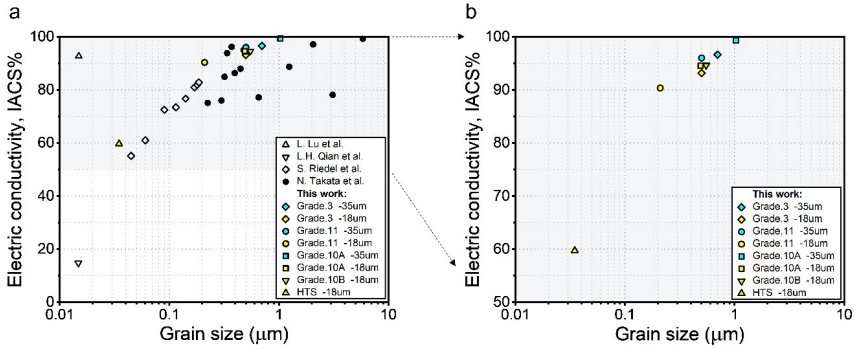

Figure 2. (**a**) Electrical conductivity as a function of cross-section grain sizes and the literature references. (**b**) A magnified region with data only from this work. Electrical conductivity is expressed to the conductivity of the International Annealed Copper Standard (%IACS) defined as 5.8001 × 107 S/m (100 %IACS) at 20 °C..

The high-resolution TEM imaging of grain and twin boundary under the same observation zone axis is achieved and the differences in terms of atomic arrangements, clearly reveal the lack of atomic positioning distortions along the twin interface. The difference precisely in terms of atomic positions on these two types of interfaces is the underlying mechanism of Cu foil microstructure control.

The knowledge obtained in this work provides valuable insights for modification of foil properties through control of microstructure interfaces.

Study Of the Intergranular Liquefaction Behavior of Precipitation Strengthened Nickel Based Superalloys

Dongting Wu[1], Yue Liu[1], Zhenhuan Gao[2], Xiufang Gong[2], Yong Zou[1,3*]

[1]*MOE Key Laboratory for Liquid-Solid Structure Evolution and Processing of Materials, Shandong University, Jinan, Shandong, China*

[2]*National Key Laboratory of Clean and Efficient Turbine Power Equipment, Dongfang Turbine Co., Ltd. of Dongfang Electric Corporation, Deyang, Sichuan, China*

[3]*Shandong Engineering & Technology Research Center for Modern Welding, Shandong University, Jinan, Shandong, China*

**Corresponding author: yzou@sdu.edu.cn*

In order to reveal the intrinsic cause of liquefaction crack formation during the welding process of precipitation strengthened nickel-based superalloys, the present study is conducted to thoroughly investigate the intergranular liquefaction behaviour of Mar-M247 nickel-based superalloy through thermal simulation experiments. It is found that when the peak temperature of the thermal simulation reaches 1160°C, the ɣ′ phase starts to appear dissolution phenomenon. With the increase of temperature, when the peak temperature reaches 1250°C and the holding time is only 0.5s, the γ′ phase undergoes extensive dissolution and component liquefaction. At the peak temperature of 1250°C, a liquefied film appears at the grain boundary and micropores appear in the thermal simulation. As the temperature continues to increase, the size of the continuous liquid film increases at a peak temperature of 1300°C and liquefaction cracks are induced, confirming the origin of the HAZ intergranular liquid film. At the peak temperature of 1320 °C for the thermal simulation, the γ′ phase was completely dissolved, but no obvious liquid film structure was observed, instead a large number of shrinkage cracks induced by grain boundary melting appeared

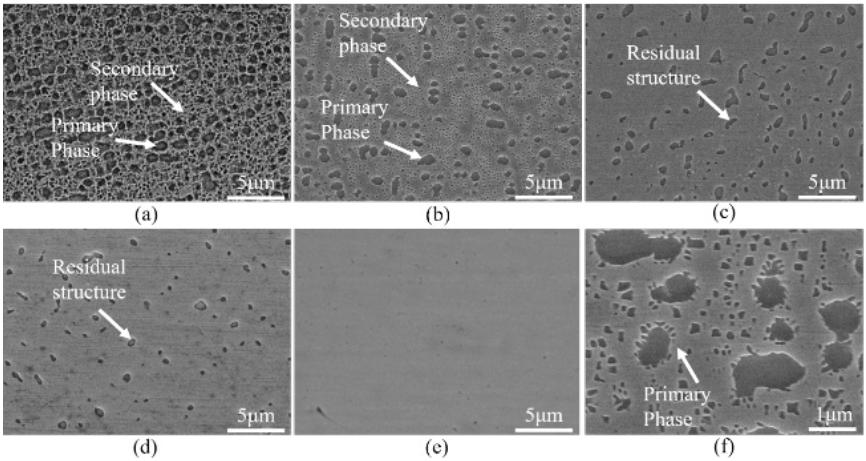

Figure 1. Intragranular organization of thermally simulated samples (**a**) 520°C (**b**) 1160°C (**c**) 1250°C (**d**) 1300°C (**e**) 1320°C (**f**) Local enlargement (1160°C)

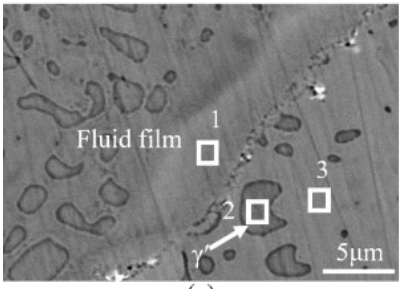

No.	Ni	Al	Ti	Cr	Co
1	60.49	5.10	0.94	9.42	9.72
2	59.21	4.63	1.04	9.50	10.46
3	60.93	5.03	1.11	8.69	9.54
No.	Mo	Ta	Hf	W	
1	0.58	3.51	0.09	6.33	
2	0.70	3.69	0.69	6.0	
3	0.56	3.39	0.57	5.21	

(b)

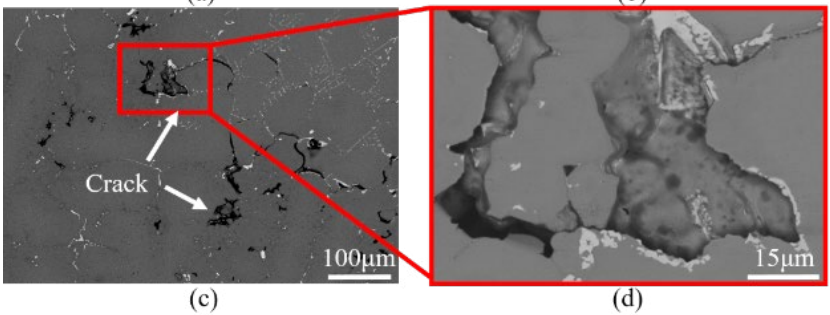

Figure 2. Intergranular liquid film and cracks (**a**) Intergranular liquid film (1250°C) (**b**) EDS analysis of liquid film composition (1250°C) (**c**) Shrinkage cracks (1320°C) (**d**) Localized magnified view (1320°C)

Solidification Segregation-Derived Heterostructure Formation in Titanium-Iron Alloy

Takuya ISHIMOTO[1*], Rio YOSHIDA[2], Tomoyo MANAKA[1], Kazuhisa SATO[3]

[1]*Aluminium Research Center, University of Toyama, Toyama, Toyama, Japan*

[2]*Graduate School of Science and Engineering, University of Toyama, Toyama, Japan*

[3]*Research Center for Ultra-High Voltage Electron Microscopy, Osaka University, Ibaraki, Osaka, Japan*

**Corresponding author: ishimoto@sus.u-toyama.ac.jp*

The introduction of heterogeneity in microstructures is a promising strategy for overcoming the tradeoff between strength and ductility in metallic materials. We attempted to introduce heterostructures into Ti-Fe binary alloys by utilizing segregation during solidification, although solidification segregation is usually eliminated by solution treatment.

Ti-Fe alloy ingots were prepared via vacuum arc melting. The ingot was aged according to compositional partitioning. Phase, microstructures, and compositional distribution before and aging were analyzed by XRD, SEM, TEM, STEM, and EDS. The mechanical properties were evaluated using Vickers hardness and compression tests.

After solidification, the segregation-derived modulation of the composition was observed. After aging heat treatment, heterostructures were formed (Fig. 1). The specimen exhibited an improved balance between strength and fracture strain compared with the specimens in which segregation was eliminated by solution treatment.

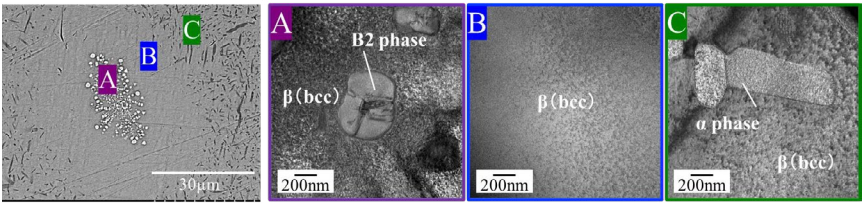

Figure 1. Formation of heterostructures with three types of regions.

Development of New Alloys for Biomaterials by Solvent Multicomponentization of Metastable Beta Ti Alloys

Yusuke NOMURA[1], Tomoyo MANAKA[2], Taiki TSUCHIYA[1], Mami IWASAKI[2], Kenji MATSUDA[1], Takuya ISHIMOTO[2*]

[1]*Graduate School of Science and Engineering, University of Toyama, Toyama, Japan*

[2]*Aluminium Research Center, University of Toyama, Toyama, Toyama, Japan*

**Corresponding author: ishimoto@sus.u-toyama.ac.jp*

In orthopedics and dentistry, there is an urgent need to obtain low-stiffness implants that suppress stress shielding. In this study, we aimed to design alloys with increased strength while maintaining a low Young's modulus based on a metastable β-Ti alloy. We designed alloys in which Ti was partially replaced by Zr, based on ISO-approved metastable Ti-15Mo-5Zr-3Al.

All the alloys produced by arc melting and subsequent solution treatment exhibited a single β-phase solid solution, and no ω-phase was observed. The alloys exhibited a low Young's modulus equivalent to that of Ti-15Mo-5Zr-3Al and a high strength superior to that of Ti-15Mo-5Zr-3Al and Ti-6Al-4V. This strengthening was presumed to be due to solid-solution strengthening. The biocompatibility of the alloys was as good as or better than that of Ti-6Al-4V.

This research was funded by the JSPS, grant numbers JP24K01194 and JP21H05197.

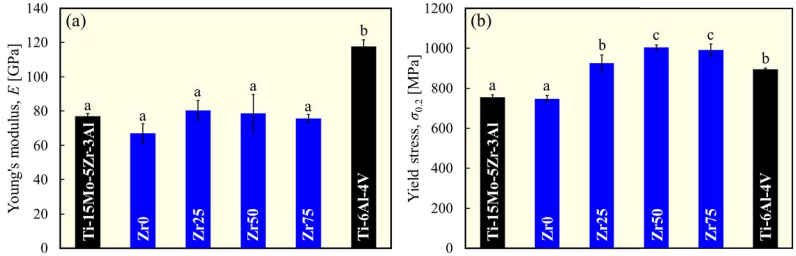

Figure 1. Variation in (**a**) Young's modulus and (**b**) yield stress of each alloy obtained from compression tests. a, b, and c indicate statistically homogeneous subgroups ($P > 0.05$, Tukey's HSD multiple comparison test).

Structures and Properties of High-Entropy Oxide-based Ceramic/Metallic Layered Systems for SOFC Interconnects

Miroslaw STYGAR[1*], Ewa DURDA[1], Marek ZAJUSZ[1], Kenji MATSUDA[2]

[1]*AGH University of Science and Technology, Faculty of Materials Science and Ceramics, Kraków, Poland*

[2]*University of Toyama, Faculty of Sustainable Design, Toyama, Japan*

**Corresponding author: stygar@agh.edu.pl*

The functional properties, including ionic conductivity, magnetic and electrical properties, thermomechanical behavior, and catalytic activity, are explored through selected examples of synthesized compositions. Design rules for these HEOx systems are formulated based on available experimental data, and the potential of these materials is assessed in comparison to their conventional counterparts, identifying distinct features resulting from the multicomponent, high-entropy arrangement of ions. Limitations are also acknowledged, indicating that not all research directions in HEOx are currently viable. In particular, the synthesis, structure, and properties of high-entropy

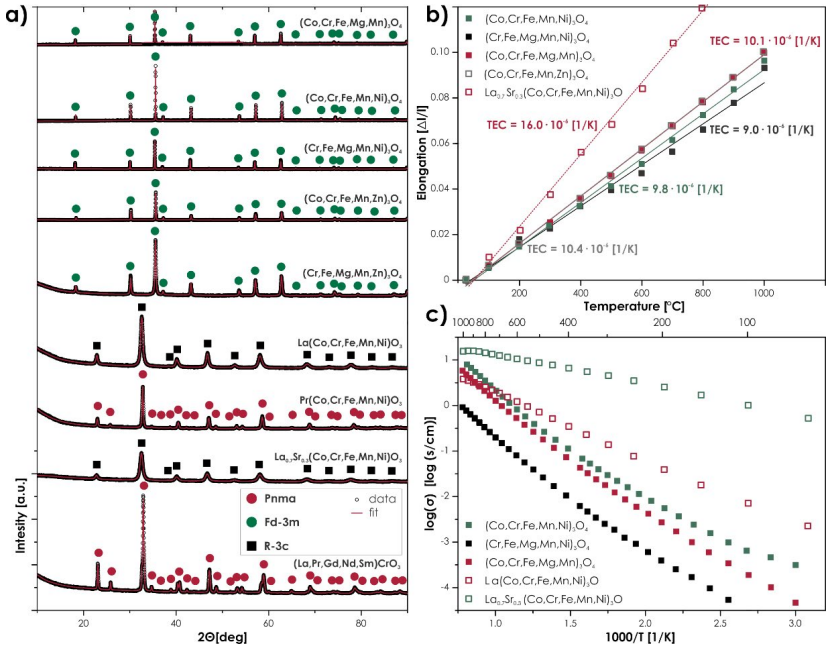

Figure 1. Exemplary data: (**a**) XRD diffraction patterns of the selected compositions obtained during preliminary studies; (**b**) total electrical conductivity for selected HEOx systems; (**c**) TEC for selected HEOx systems

spinels from the Co-Cr-Fe-Mg-Mn-Ni-O system are examined. Single-phase spinels, such as (Co,Cr,Fe,Mn,Ni)3O4, and selected quaternary subsystems are obtained, with stability evaluations showing the impact of temperature and oxygen partial pressure on spinel formation. Thermomechanical behavior is consistent across compositions, with thermal expansion coefficients compatible with solid oxide fuel cell (SOFC) technology. The electrical conductivity of these spinels reveals a semiconducting character with a notable activation energy change around 400°C. Further insights into cationic occupancy within the lattice sites are provided through Mossbauer spectroscopy and DFT calculations, revealing different tendencies between quaternary subsystems and the quinary composition.

The potential application of these high-entropy spinels as protective-conductive coatings for SOFC interconnects is proposed, highlighting their potential for corrosion protection and suppression of Cr-poisoning. Initial studies on applying such coatings on Crofer 22APU ferritic stainless steel substrates and preliminary performance assessments of the ceramic/metallic system are also presented. The abstract concludes by emphasizing the promising features of high-entropy systems for SOFC technology, while acknowledging the challenges and limitations in their current development stage.

Acknowledgments
This research was supported by the Polish National Science Center (NCN) under project Opus No. 2021/41/B/ST8/03928.

DSC Analysis as a Tool for Determining Reaction Temperatures in Welded Joints

Jan RONCAK[1*], Patrik JOZEFOVIC[2], Ondrej ADAM[3], Jakub JUDAS[3], Vit JAN[3], Martin ZOBAC[4]

[1]*TESCAN GROUP, a.s., Brno, Czechia*

[2]*Department of Control and Instrumentation, Brno University of Technology, Brno, Czechia.*

[3]*Department of Materials Science and Engineering, Brno University of Technology, Brno, Czechia.*

[4]*Group of Electron Beam Technology, Institute of Scientific Instruments of the Czech Academy of Science, Brno, Czechia.*

**Corresponding author: jan.roncak@tescan.com*

Continuous improvements in the industry and new application possibilities bring more demanding requirements for the properties of the materials under investigation. One of them is the stability of the microstructure at elevated temperatures, which guarantees the constancy of the mechanical properties. One of the studied alloys (with respect to microstructure stability) is also $AlCoCrFeNi_{2.1}$ belonging to the group of eutectic high-entropy alloys. The alloy should retain a combination of increased strength and sufficient ductility over a wide temperature range due to its high entropy. However, experimental evaluation with respect to a wide temperature variability does not allow an effective time verification of the material behavior. This can be simplified by a thermal analysis, which will determine the range of reactions of the material and thus ease the selection of the temperature for heat treatment.

The paper therefore discusses the possibility of using DSC thermal analysis (Figure 1) in determining the reaction temperatures of new materials and improving the efficiency of the evaluation process. The temperatures determined by thermal analysis were used for long-term heat treatment. Changes in the material in the form of phase transformations were verified by observation in SEM, EDS chemical and EBSD phase analysis (Figure 2). The resulting mechanical properties were determined in the form of hardness HV0.1 and tensile strength. For all tested samples, changes correlated with the reactions highlighted by DSC analysis.

The research was conducted with the institutional support RVO:68081731.

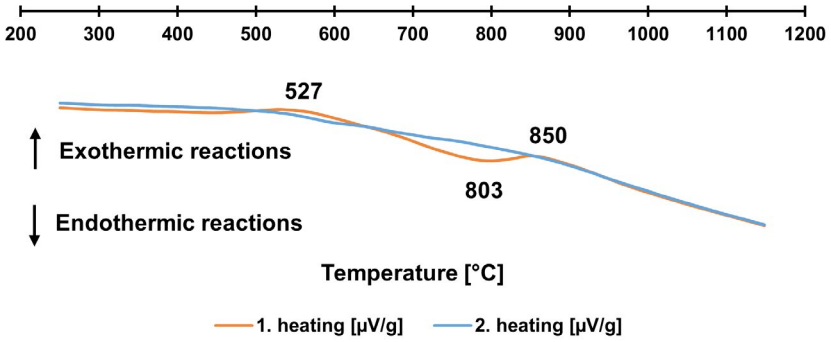

Figure 1. DSC curve of the analyzed $AlCoCrFeNi_{2.1}$ welded joint with highlighted temperatures.

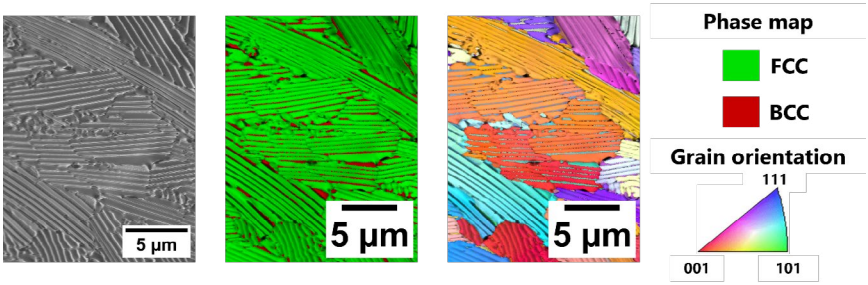

Figure 2. SEM microstructure, phase map and lamella orientation of $AlCoCrFeNi_{2.1}$ weld joint.

Physicochemical properties of the layered steel/ceramic systems for interconnect application in Proton Ceramic Fuel Cells

Ewa DURDA[1*], Miroslaw STYGAR[1], Marek ZAJUSZ[1]

[1]*Department of Physical Chemistry and Modelling, Faculty of Materials Science and Ceramics, AGH University of Krakow, Krakow, Poland*

**Corresponding author: edurda@agh.edu.pl*

Steel surface modification using spinel oxide coatings for use as an interconnect in Proton Conducting Fuel Cell (PCFC) was evaluated. As coating materials, oxides with a spinel structure from the Mn-Co and Mn-Co-Cu systems were used. Coatings were applied on the Crofer 22 APU steel using the electrophoresis method.

The samples were oxidized in an atmosphere of air containing water vapor at 600°C under isothermal conditions for 500 hours. In the case of unmodified steel (Fig. 1a), the formation of a thick, Fe-rich oxide scale occurred. On the other hand, the spinel coating had a positive impact on limiting the oxidation of the steel under tested conditions (the sample morphology was similar to that before the oxidation process). The area-specific resistance value at 600°C for Crofer 22 APU was 0.26 Ω·cm, significantly exceeding the established limit for materials intended for use as interconnectors (0.1 Ω·cm) (Fig. 1c). However, for the sample with the MCCu coating, the ASR value was significantly lower, and was equal to 0.01 Ω·cm.

In summary, Crofer 22 APU with a spinel coating obtained by electrophoresis is a very promising solution for use as an interconnect in PCFC.

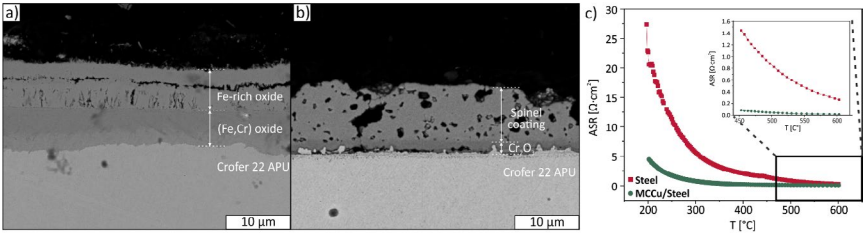

Figure 1. Cross-sectional SEM photographs of Crofer 22 APU (**a**) and Crofer 22 APU with MCCu spinel coating (**b**) after oxidation in humidified air for 500 h at 600°C; temperature dependence of ASR for the pure Crofer 22 APU steel and the Crofer 22 APU/MCCu composite (**c**).

CHAPTER II

The Effect of pH, Concentration and Temperature Of Electrolyte For Uniform Gold Electrodeposition

Tung Do Cuong[1], Injoon Son[1*]

[1]*Department of Materials Science and Metallurgical Engineering Kyungpook National University, Daegu 41566, Republic of Korea*

**Corresponding author: ijson@knu.ac.kr*

Steel surface modification using spinel oxide coatings for use as an interconnect in Proton Conducting Fuel Cell (PCFC) was evaluated. As coating materials, oxides with a spinel structure from the Mn-Co and Mn-Co-Cu systems were used. Coatings were applied on the Crofer 22 APU steel using the electrophoresis method.

The samples were oxidized in an atmosphere of air containing water vapor at 600°C under isothermal conditions for 500 hours. In the case of unmodified steel (Fig. 1a), the formation of a thick, Fe-rich oxide scale occurred. On the other hand, the spinel coating had a positive impact on limiting the oxidation of the steel under tested conditions (the sample morphology was similar to that before the oxidation process). The area-specific resistance value at 600°C for Crofer 22 APU was 0.26 Ω·cm, significantly exceeding the established limit for materials intended for use as interconnectors (0.1 Ω·cm) (Fig. 1c). However, for the sample with the MCCu coating, the ASR value was significantly lower, and was equal to 0.01 Ω·cm.

In summary, Crofer 22 APU with a spinel coating obtained by electrophoresis is a very promising solution for use as an interconnect in PCFC.

Effect of the Addition of Sm to Pyrochlore-structured Potassium Tantalate on its Photocatalytic Activity

Haruka KITAHARA[1], Takashi HASHIZUME[1], Atsushi SAIKI[1*]

[1]*Materials Science and Engineering, University of TOYAMA, Toyama, Japan*

**Corresponding author: saiki@sus.u-toyama.ac.jp*

Potassium tantalate is known as a photocatalytic material that exhibits water splitting reactions and the addition of rare earth elements has been reported to improve its activity. The crystal structure of potassium tantalate has a pyrochlore structure and a perovskite structure, and the pyrochlore structure was adopted in this study due to the less restrictive nature of the added elements. However, due to the large band gap, photoexcitation reactions do not occur in the visible light region and strong UV light is required. In this study, potassium tantalate with a pyrochlore structure was doped with Sm, a rare earth element, to investigate the reduction of the band gap and the improvement of photocatalytic activity.

The hydrothermal synthesis method was used for the synthesis. As a result, potassium tantalate with Sm was synthesized. Furthermore, the addition of Sm was confirmed to reduce the band gap and improve the photocatalytic activity.

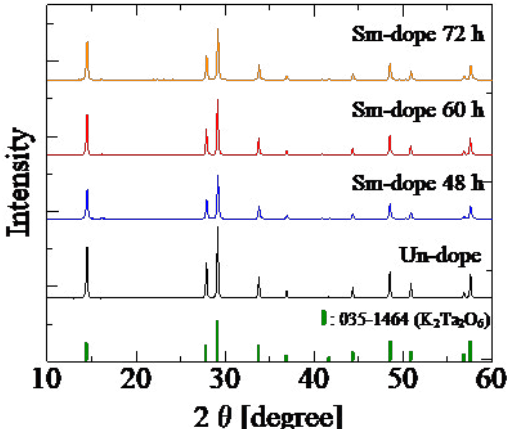

Figure 1. XRD measurements of the prepared samples.

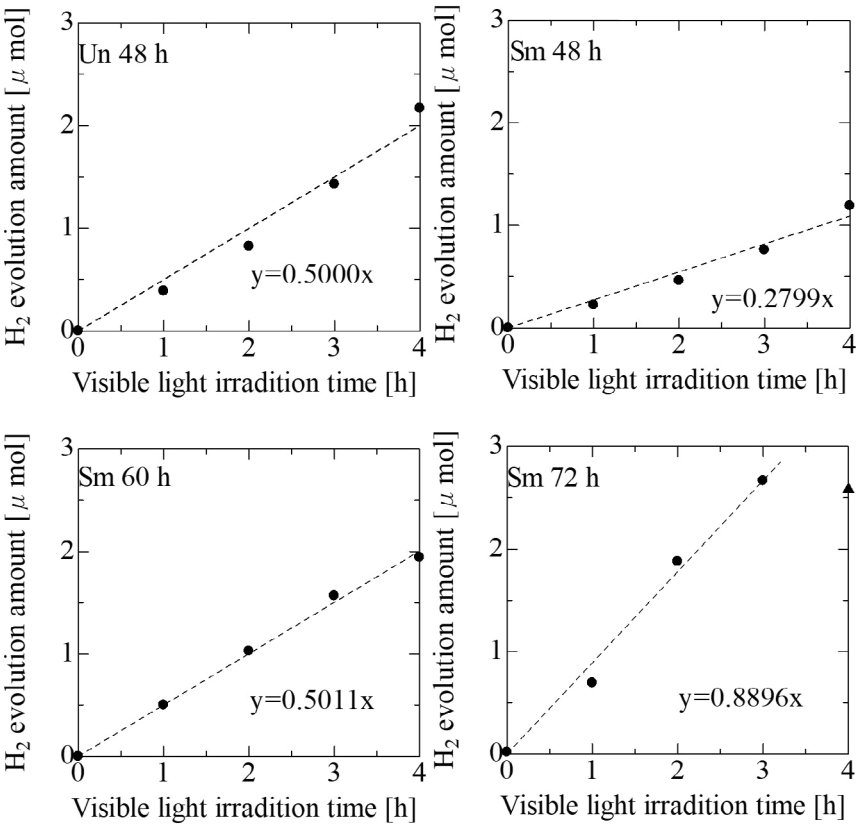

Figure 1. Measurements of the rate of hydrogen production by the batch method
▲ *indicates that the container has been saturated due to insufficient capacity*

Exothermic Reactivity of Aluminum Powders Coated With Copper And Nickel

Changgyun Kim[1], Seo young An[1], Injoon Son[1*]

[1]*Department of Metallurgical Materials Science and Engineering, Kyungpook National University*

**Corresponding author: ijson@knu.ac.kr*

Aluminum powders are used for explosives. However, it is reported that passivated oxide layer hinders the reactivity of the Aluminum powder. In this study, we replaced the oxide layer with Copper and Nickel by electroless-plating and replacement. We first removed the oxide layer of the Aluminum by etching in the hydrofluoric based acid solution. Then, we electroless-plated Copper and Nickel onto the Aluminum powders. We varied the plating time (10/20/40 min) and analyzed the plated surface with FE-SEM and EDS. Also, we compared the morphology of the Nickel-coated Aluminum powders produced by replacement method and by electroless-plating method. We tested Nickel replacement with various PH (8/9/10/11). Finally, we investigated the exothermic reaction of the passivated Aluminum, Copper coated Aluminum, Nickel coated Aluminum powders. It is assumed that Nickel or Copper coated Aluminum gained more energy because of self-propagating high-temperature synthesis (SHS) reaction between Aluminum, Copper, and Nickel

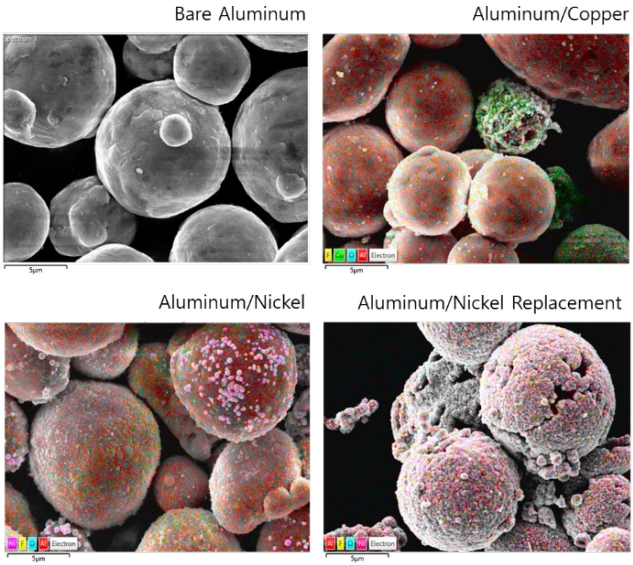

Figure 1. FE-SEM and EDS image of Copper-coated and Nickel-coated Aluminum Powders.

Hardness Improvement by Adding Bismuth in Silver Electroplating

Injoon Son[1*]

[1]*Department of Metallurgical Materials Science and Engineering, Kyungpook National University*

**Corresponding author: ijson@knu.ac.kr*

Silver electroplating is widely used in industry from the electronics to the automobile because of its good electrical conductivity. However, silver coating has low hardness compared to other metal coating. There have been attempts to improve the hardness of the Silver by alloying. We chose Bi as an alloying element to improve the hardness of electroplated Silver in this research. We investigated the mechanical property of Ag-Bi alloy before and after heat treatment. The hardness of Ag-Bi increased with Bi addition. From the XRD data, we assume that Ag-Bi hardness improved with solid-solution hardening. When the Silver layer is exposed to the heat treatment, Pure Silver hardness dropped, whereas the Ag-Bi layer maintained its hardness up to 125 °C. Also, EBSD results show the grain refinement by adding Bismuth to the silver layer. Therefore, proper combination of heat treatment temperature and Bi composition will meet the needs of both of electrical and mechanical properties in the industry.

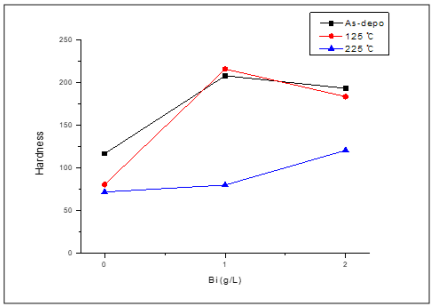

Hardness of electroplated Ag-Bi layer
(Bi amount in electroplating solution dependent)

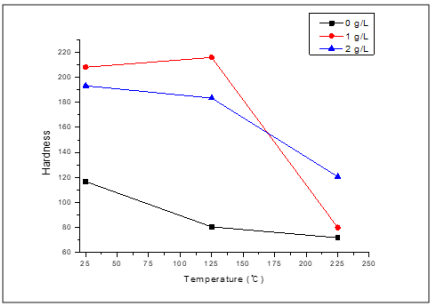

Hardness of electroplated Ag-Bi layer
(Temperature dependent)

Figure 1. Hardness change of electroplated Ag-Bi layer with Bismuth concentration and Temperature.

Analyses of Phase Stability, Microstructure, and Mechanical Properties of Laser Powder Bed Fusion-Produced Ti-6Al-4V/ Ti-15Mo-5Zr-3Al Interface

Sho MAEGAWA[1*], Ryuto OKAZAKI[2], Tomoyo MANAKA[3], Takuya ISHIMOTO[3*], Takayoshi NAKANO[4]

[1]Graduate School of Science and Engineering, University of Toyama, Toyama, Japan

[2]School of Sustainable Design, University of Toyama, Toyama, Japan

[3]Aluminium Research Center, University of Toyama, Toyama, Japan

[4]Division of Materials Science and Engineering, Graduate School of Engineering, Osaka University, Osaka, Japan

**Corresponding author: ishimoto@sus.u-toyama.ac.jp*

Multimaterial devices with different functionalities in a single structure are beneficial for biomaterials. The purpose of this study is to clarify the properties of the interface between α+β-type Ti-6Al-4V and β-type Ti-15Mo-5Zr-3Al. The specimens were prepared by the laser powder bed fusion (LPBF) of Ti-15Mo-5Zr-3Al on a Ti-6Al-4V substrate. The composition at the interface transitioned toward a composition of Ti-15Mo-5Zr-3Al in a distance-dependent manner from the Ti-6Al-4V substrate. The Mo equivalent, α/β transformation point, and constituent phases were changed accordingly. The Vickers hardness of the interface region was higher than those of the Ti-6Al-4V and Ti-15Mo-5Zr-3Al regions. In the tensile tests involving the interface, ductile fracture occurred, indicating the mechanical stability of the interface. No strength loss occurred at the interface, suggesting that it was functionally fused.

This research was funded by the JSPS, grant numbers JP24K01194 and JP21H05197.

Soft Magnetic Properties of Fe-based Amorphous Core Prepared by Various Sintering Methods

Hyungjin Nam[1], Seongjun kim[1], Eunjin Park[1], Seonghoon Yi[1*]

[1]School of Materials Science and Engineering, Department of Materials Science and Metallurgical Engineering, Kyungpook National University, Daegu, Korea.

**Corresponding author: yish@knu.ac.kr*

Soft magnetic materials have attracted significant attention in various industries due to their exceptional magnetic properties and wide-ranging applications. With the growing demand for miniaturization, these materials have become increasingly important. Characterized by high permeability, low hysteresis loss, and high saturation magnetization, soft magnetic materials are ideal for advanced technological applications. Unlike crystalline structures, amorphous materials offer enhanced yield strength and corrosion resistance, making them particularly advantageous.

In this study, amorphous ribbons were fabricated using the melt-spinning technique, followed by milling to produce fine flakes for the sintering process. The amorphous state was confirmed through X-ray diffraction (XRD) and differential thermal analysis (DTA). Sintering was conducted via spark plasma sintering (SPS) and hot press sintering, both selected to preserve the amorphous structure and optimize magnetic properties. The primary objective was to maintain stable permeability and high magnetic performance in the high-frequency range.

Magnetic properties of the amorphous toroidal cores were evaluated using vibrating sample magnetometry (VSM), DC tracer, and AC analysis. The results confirmed that the materials exhibited excellent soft magnetic properties, validating their potential for high-frequency applications in advanced soft magnetic devices.

Soft magnetic properties of Fe-Si-C-P amorphous ribbons

Seunghoon Yi[1*], Moosung Kim[1], Sejin Jang[1]

[1]*School of Materials Science and Engineering, Department of Materials Science and Metallurgical Engineering, Kyungpook National University, Daegu, Korea.*

**Corresponding author: yish@knu.ac.kr*

Soft magnetic materials play a crucial role in various electronic applications due to their excellent magnetic properties. In this study, we investigate the soft magnetic properties of Fe-Si-C-P amorphous ribbons with enhanced glass-forming ability (GFA) and tailored magnetic characteristics. The compositions were designed with relatively high phosphorus (P) and carbon (C) content in iron (Fe) base. By incorporating high levels of P and C, several advantages emerge. For instance, it enhances ductility and flexibility, improve corrosion and oxidation resistance, and enables cost-effective production due to the availability and affordability of these elements.

The alloys were synthesized via arc-melting followed by melt-spinning to produce flexible ribbons. The microstructural evaluation was conducted using techniques such as X-ray diffraction (XRD) to confirm the amorphous nature and scanning electron microscopy (SEM) for microstructure observation. Thermal analysis was carried out using simultaneous differential thermal analysis (SDT). The magnetic properties were characterized using vibrating sample magnetometry (VSM) loop to measure magnetization density, coercivity etc. Our results demonstrate the feasibility of tailoring soft magnetic properties in Fe-Si-C-P amorphous ribbons through precise composition design and processing techniques.

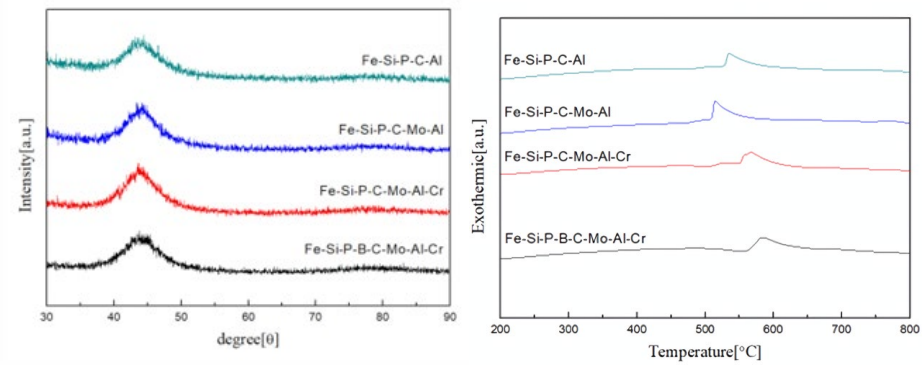

Figure 1. Thermal, XRD Analysis

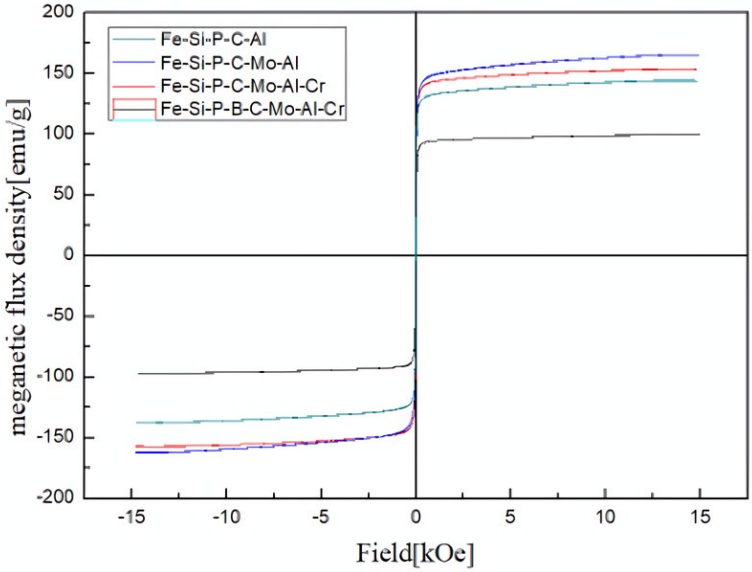

Figure 2. Magnetic analysis

Reduction Behavior of NCM-Based Lithium-Ion Battery Cathode Materials by CO and Li Recovery by Water Leaching

Sang-Yeop Lee[1], Jae-Ho Hwang[1], So-Yeong Lee[1], Ho-Sang Sohn[1*]

[1]Kyungpook National University, Department of Materials Science and Metallurgical Engineering, Daegu, Republic of Korea

**Corresponding author: sohn@knu.ac.kr*

Efforts to combat the climate crisis are driving a shift from fossil fuels to green energy, rapidly growing the electric vehicle market. Lithium, essential for EVs, is in high demand. Recovering lithium from spent $Li(Ni_xCo_yMn_z)O_2$ (NCM) batteries is crucial, with reduction roasting using CO gas being an effective method.

The samples were heated to 1,000°C in step of 100°C, monitoring weight changes and exhaust gas concentrations in real time at Ar and Ar-CO atmosphere. The roasted samples were water-leached, and the leachate was dried to recover lithium as Li_2CO_3 powder.

Above 600°C, Ni and Co are fully reduced to metallic forms by CO gas. But Mn remained in oxide because of thermodynamically impossible to reduced. Li_2CO_3 was synthesized by reacting Li_2O with CO_2 gas above 500°C. Leaching experiments show that higher reduction roasting temperatures improve lithium recovery rates. The highest recovery rates were achieved at reduction roasting temperatures of 700°C and 800°C, with recovery rates exceeding 90% and purity over 98%.

Investigation of crystallization behavior and magnetic property changes of Fe-P-B-Si-C-Cu alloys under heat treatment

Eunjin Park[1], Hyungjin Nam[1], Seonghoon Yi[1*]

[1]School of Materials Science and Engineering, Department of Materials Science and Metallurgical Engineering, Kyungpook National University, Daegu, Korea.

**Corresponding author: yish@knu.ac.kr*

Fe-based soft magnetic amorphous alloys have attracted tremendous interest in both academia and industry due to their high efficiency and low core loss when used as core materials in transformers and motors. In this study, we investigated the crystallization behavior and magnetic property changes of the Fe-P-B-Si-C-Cu alloy under various heat treatment conditions. Amorphous ribbons were prepared using arc melting and melt spinning techniques, followed by annealing at different temperatures and durations. Characterization was performed using X-ray diffraction (XRD), Thermal analysis (SDT), VSM, and DC BH tracer loop measurements. Results showed that heat treatment induced crystallization with the formation of α-Fe phases. Magnetic properties, such as coercivity and saturation magnetization, varied with heat treatment conditions, indicating the critical role of annealing parameters. It is essential to determine the optimal heat treatment conditions to achieve desirable magnetic properties by balancing coercivity and saturation magnetization. This study successfully identified the optimal heat treatment conditions for achieving these balanced properties.

CHAPTER III

Development of lead-free solder paste material containing cellulose nanofibers

Tetsuya AIDA[1*]

[1]*Department of Sustainable Design, University of Toyama, Toyama, Japan*

**Corresponding author: aida@sus.u-toyama.ac.jp*

In recent years, environmental concerns have been growing on a global scale from the perspective of protecting the global environment. The solder that has been mainly used for mounting boards for electronic devices is an alloy of tin (Sn) and lead (Pb). However, when acid rain falls on discarded electronic devices, the lead oxide formed on the solder surface dissolves due to the nitric acid components of the acid rain, causing contamination and adverse effects on the human body, which has become a problem.

As a result, Sn-Ag-Cu lead-free solder is mainly used as a lead-free solder to replace Sn-Pb eutectic solder. Sn-Ag-Cu lead-free solder has excellent mechanical properties and high joint reliability, but it has problems such as a melting point of 219°C, which is higher than the 183°C of Sn-Pb eutectic solder, a high defect (void) density, and poor wettability.

In this study, we added cellulose nanofibers (CNFs), a nano-sized material, to Sn-3. 0mass%Ag-0.5mass%Cu-based lead-free solder to improve mechanical properties and reduce voids, and investigated the effect of adding CNFs to the shear strength.

CNFs are nano-sized fibrous materials extracted from cellulose fibers obtained from wood through mechanical and chemical processing. They are known as nano-sized materials with fiber widths ranging from a few nm to a few tens of nm, and have characteristics such as high strength, high elasticity, and low linear thermal expansion.

In this study, we used CNFs prepared by the underwater counter collision method (ACC method). The underwater counter collision method uses shear energy generated by high-speed counter-collision collision of water-suspended samples to preferentially defibrate weak intermolecular interactions, resulting in fiber diameters of several nm to 10 nm, which are thicker than those obtained by chemical processing, which produces fiber diameters of about 3-5 nm. Due to these characteristics, the ACC method is suitable for joining solder heated to about 260°C, and we found the possibility that CNFs may remain in the solder fillet while maintaining their properties even after joining by reflow.

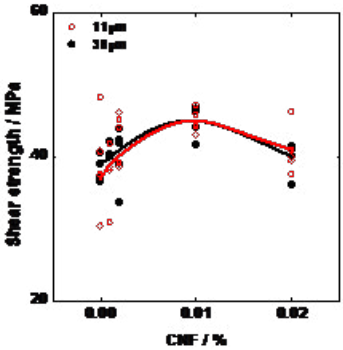

Figure 1. Relationship between CNF additional amount and shear strength.

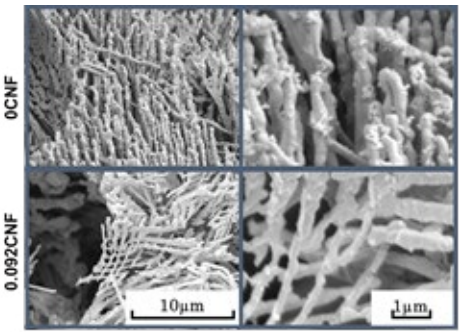

Figure 2. SEM observation image.

Metamagnetic phase transition induced large magnetocaloric effect

Wanting YANG[1], Shixun CAO[1,2*], Mathias KLÄUI[3-5*]

[1]*Department of Physics, Materials Genome Institute and International Center for Quantum and Molecular Structures, Shanghai University, Shanghai, 200444, China.*

[2]*Shanghai Key Laboratory of High Temperature Superconductors, Shanghai University, Shanghai, 200444, China.*

[3]*Institute of Physics, Johannes Gutenberg University Mainz, Staudingerweg 7, 55128 Mainz, Germany.*

[4]*Graduate School of Excellence Materials Science in Mainz, Staudingerweg 9, 55128 Mainz, Germany.*

[5]*Center for Quantum Spintronics, Norwegian University of Science and Technology, Trondheim 7491, Norway.*

**Corresponding author: sxcao@shu.edu.cn, Klaeui@Uni-Mainz.de*

$DyFeO_3$ exhibits strong antiferromagnetic coupling in all directions, while $DyMnO_3$ shows dominant FM-e_g^1-O-e_g^0 interaction of in the *ab* plane. We introduced Mn ions into Fe sites of $DyFeO_3$ at 10%–50% ratios to coexist antiferromagnetic and ferromagnetic coupling in the *ab* plane. In half-doped crystal, the magnetic configuration of Dy sublattices changes, resulting in a significant magnetocaloric effect. The negative magnetic entropy change along the *c*-axis approaches 10.41 J/kg K at 5 K under 0–70 kOe (compared to 0 J/kg K for $DyFeO_3$, 0.93 J/kg K for orthorhombic $DyMnO_3$), and the refrigeration capacity reaches 84.63 J/kg, correspondingly. The spin configuration of Dy^+ shifts from Γ_5 (G_x, A_y) to Γ_4 (F_z), increasing the ferromagnetic component along the *c*-axis. On the other hand, the large adiabatic temperature change, contributed by magnons, indicates exceptional refrigeration efficiency in a direct way. Therefore, it is possible to convert $DyFeO_3$ into a magnetic refrigeration contender at low temperatures.

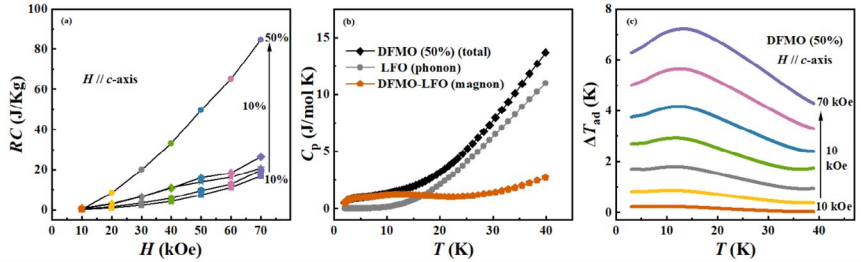

Figure 1. Refrigeration capacity and adiabatic temperature change. (**a**) Magnetic fields dependences of the refrigeration capacity of DFMO (10 %–50 %) along *c*-axis. (**b**) Temperature dependence of the zero-field heat capacity of DFMO (50 %), LFO ($LuFeO_3$) and their difference. (**c**) Adiabatic temperature change of DFMO (50 %) driven by magnons along c-axis calculated by the magnetic heat capacity and magnetic entropy change.

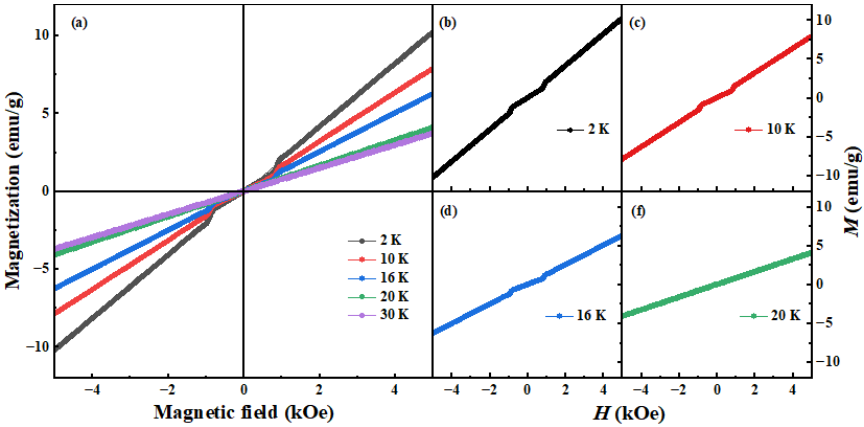

Figure 1. Metamagnetic phase transition. (**a**) *M-H* curves of DFMO (50 %) single crystal along *c*-axis at 2, 10, 16, 20, 30 K. (**b–d**) *M-H* curves at 2, 10, 16 and 20 K, respectively.

Superconductng properies of $Zr_2(Co_{1-x}T_x)$ (T = Pd, Pt)

Takahiro NAMIKI[1*], Yoshiki HACHIYA[2], Ryunosuke KOBATA[1], Takuya OHASHI[1], Daisuke TSURUSE[1], Katsuhiko NISHIMURA[1]

[1]*Department of Materials Design and Engineering, School of Sustainable Design, University of Toyama, Toyama, Japan.*

[2]*Graduate School of Science and Engineering, University of Toyama, Toyama, Japan.*

**Corresponding author: namiki@sus.u-toyama.ac.jp*

Electrical resistivity (ρ), magnetization (M), and specific heat (C) measurements of pseudo-binary alloyed compounds $Zr_2(Co_{1-xTx})$ (T = Pd or Pt) were done to investigate the substitution effect on the superconducting properties. The superconducting transition temperature (T_c) of Zr_2Co was observed at 5.6 K, which agrees with the previously reported one [1]. The substations of Pd or Pt for the Co site were found to bring about positive effects; the critical temperature (T_c), the critical field (H_{c2}), and the critical current density (J_c) increased with increasing the Pd or Pt contents. The electronic specific heat coefficients (γ_e) and the superconducting energy gaps (Δ) deduced from the C measurements also increased with the substitution, that is, the γ_e and Δ values are in a linear relationship with the T_c values.

The polycrystalline samples were prepared by arc melting method. The crystal structure of the prepared sample was confirmed to be of the body-centered tetragonal structure ($CuAl_2$-type, I4/*mcm*, No. 140) from the X-ray diffraction patterns, providing the lattice constants of a = 6.3969 Å and c = 5.523 Å for Zr_2Co, which are in good agreement with the literature values [2]. The lattice constants of $Zr_2(Co_{1-x}Pd_x)$ increased with increasing x; for Zr*2*(Co*1-x*Pt*x*), the a values increased but the c values decreased with x.

Figure 1 shows the temperature dependences of ρ for Zr_2Co, $Zr_2Co_{1-x}Pd_x$. The ρ vs T curves monotonically decreased with temperature. The superconducting transitions of the samples were observed, at Tc = 5.6 K, 6.4 K, and 6.7 K for Zr_2Co, $Zr_2Co_{0.9}Pd_{0.1}$, and $Zr_2Co_{0.9}Pt_{0.1}$, respectively. From the ρ data, we evaluated the residual resistivity ratio (RRR) by ρ(300K)/ρ(10K) to be 64 for Zr_2Co, which indicates a high quality of the sample [3]. As shown in Figure 2, from the determined T_c-vs-H_{c2} phase diagram, H_{c2} were extracted to be 1.6 T, 5.5 T, and 4.5 T for Zr_2Co, $Zr_2Co_{0.9}Pd_{0.1}$, and $Zr_2Co_{0.9}Pt_{0.1}$, respectively; the substitution effect on H_{c2} are very large. More detailed results and analyses including M and C will be presented at the conference.

[1] Z. Fisk et al., Solid State Commun. 15 1797 (1974).
[2] S. L. McCarthy, J. Low Temp. Phys. 4 489 (1971).
[3] A. Teruya et al., J. Phys. Soc. Jpn. 85 034706 (2016).

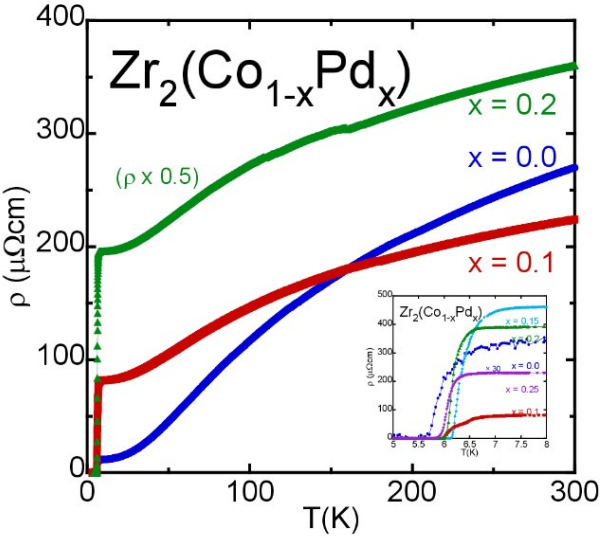

Figure 1. The temperature dependences of the resistivity (ρ) for ($Co_{1-x}Pd_x$). Inset shows the ρ around the transition temperature.

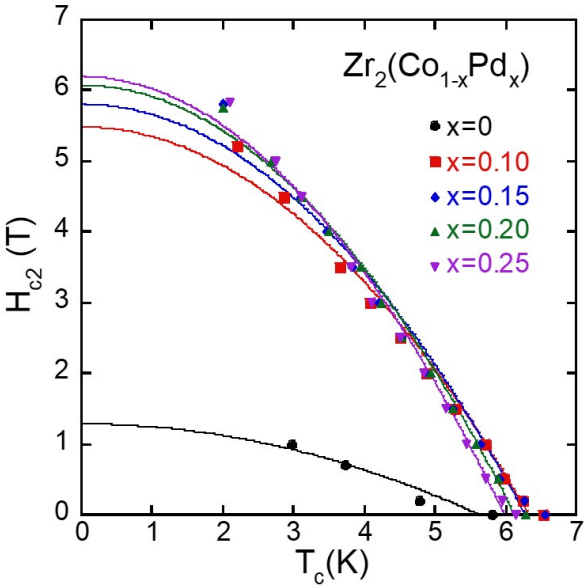

Figure 2. The determined T_c-vs-H_{c2} phase diagram of $Zr_2(Co_{1-x}Pd_x)$

Si Removal from Molten Aluminum through Liquid-Liquid Partitioning Using Molten Sodium

Kengo KATO[1*], Takuma TSUBOI[2], Hideki ONO[1]

[1]*Academic Assembly, Faculty of Sustainable Design, University of Toyama, Toyama, Japan*

[2]*School of Sustainable Design, University of Toyama, Toyama, Japan.*

**Corresponding author: kato@sus.u-toyama.ac.jp*

The smelting process of aluminum ore requires a large quantity of electric energy, whereas themelting and recycling of used aluminum products consumes less energy. Therefore, aluminumrecycling can reduce energy consumption to not more than 1/10 of primary aluminum production.Accordingly, the recycling of aluminum is a critical issue to achieve carbon neutrality. However,impurity elements are inevitably contained in the Al scrap recovered from society, and most ofthem are difficult to remove by the current pyro-metallurgical processes. Therefore, thealuminum scraps are mainly recycled into the cast alloys which has a high tolerance level ofimpurities. Silicon is usually added to cast Al alloy to improve the fluidity of molten aluminumwhereas the silicon content of wrought aluminum alloy is controlled to be less than 1 mass%.Therefore, silicon removal is necessary to recycle cast aluminum scraps into wrought aluminumalloys. On the other hand, sodium forms intermetallic compounds with silicon although it isimmiscible with Al, which suggests that the attractive interaction works between sodium andsilicon. In this study, silicon removal from molten aluminum through liquid-liquid partitioningusing molten sodium was proposed. The concept of the silicon removal is schematicallyillustrated in Fig. 1. Two immiscible phases of molten aluminum and molten sodium coexist athigh temperatures and silicon in molten aluminum may be transferred to molten sodium due tothe attractive interaction between silicon and sodium. Aluminum, silicon, and sodium regentswere heated to 938 and 998 K in an Al2O3 crucible, and the silicon content of molten aluminumwas investigated. Figure 2 shows the effect of temperature on the silicon content of aluminum. Itwas found that silicon content of aluminum can be decreased from 10 mass%. The siliconcontent of aluminum was lower at 938 K than 993 K. it was confirmed that silicon can be removedfrom molten aluminum through Liquid-Liquid partitioning using molten sodium.

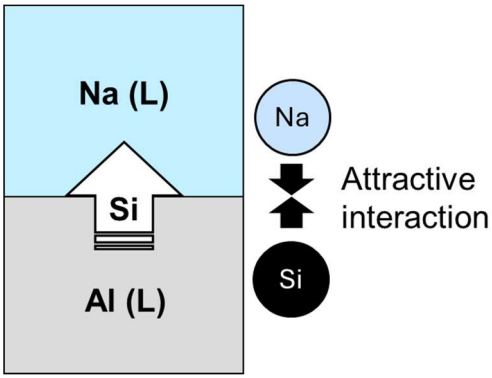

Figure 1. The concept of the silicon removal from molten aluminum through Liquid-Liquid partitioning.

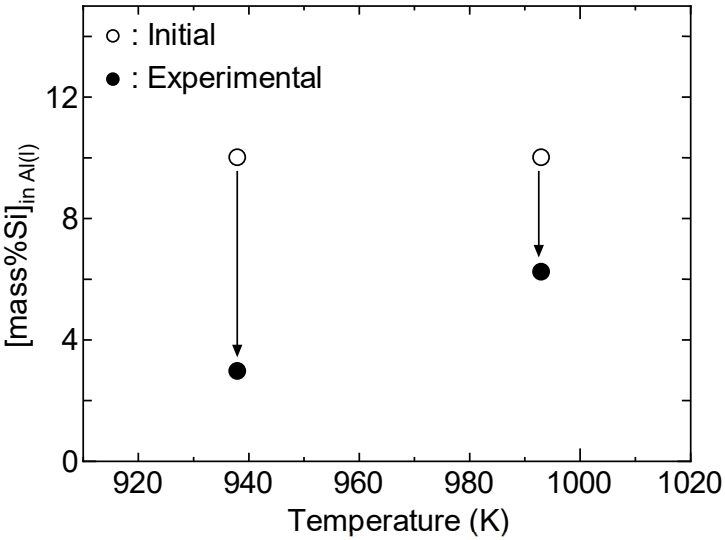

Figure 2. Effect of temperature on the silicon content of aluminum.

Image Processing Technology Toward Multi-Modal Analysis of Steels

Takashi MICHIKAWA[1], Norio YAMASHITA[1], Zhe SUN[1,2], Shin YOSHIZAWA[1], Masahiko MORITA[1], Yuuki AIDA[1,3], Shinya MORITA[1,3], Toru HARA[4], Masahiro INOMOTO[5], Yoshitomi OKAZAKI[5] and Hideo YOKOTA[1*]

[1]*RIKEN Center for Advanced Photonics, RIKEN, Saitama, JAPAN*

[2]*Faculty of Health Data Science, Juntendo University, Chiba, JAPAN*

[3]*Department of Advanced Machinery Engineering, Tokyo Denki University, Tokyo, JAPAN*

[4]*National Institute for Materials Science, Ibaraki, JAPAN*

[5]*Kobe Steel, Ltd., Hyogo, JAPAN*

**Corresponding author: hyokota@riken.jp*

We own two serial-sectioning devices for steel observation: an original optical microscope using elliptical vibration cutting, and FIB SEM. Since supporting scale and resolution are different, we obtain limited information from each imaging result. We outline three image processing techniques toward multi-modal image analysis of steels using martensite-austenite constituents (M-A) observation in high-tensile steels as an example (Figure 1). These include M-A segmentation from optical microscope images using U-Net, drift correction of stacked SEM images using phase-only correlation, and registration of optical microscope images and SEM images using voting of the results of phase-only correlation (Figure 2). By using these methods, two imaging results acquired by different resolutions, FOVs, and imaging principles can be connected in a common digital space. These results will contribute to analysis of the steel properties.

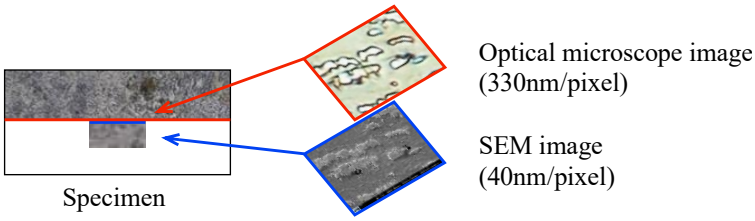

Figure 1. Our concept of image analysis with two serial-sectioning devices.

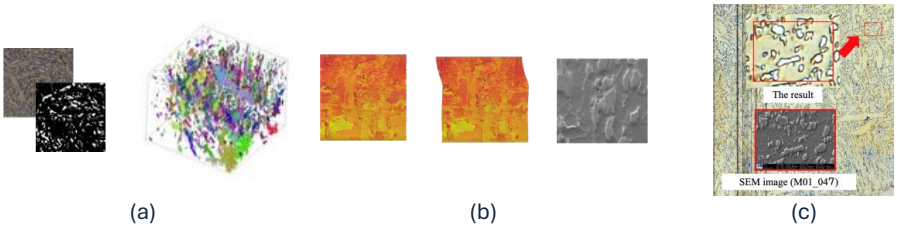

Figure 2. Our image processing technology. (**a**) M-A segmentation from optical microscope images (800x800 pixels) (left), and 3D visualization of individual M-As (right). (**b**) Drift correction of SEM images. From left to right: stacked SEM images from top-view, corrected stacked images from top view, and a reference SEM image (acquired before serial-sectioning). (**c**) Registration of SEM and optical microscope images. Our method can find the location of a SEM image (1024x768 pixels, scaled size: 113x85 pixels) in an optical microscope image (cropped, original size: 3888x5184 pixels).

Circular Line Method Application: Image Processing For Steel Industry

Martin ZOUHAR[1*], Šárka MIKMEKOVÁ[1]

[1]*Department of Electron Microscopy, Institute of Scientific Instruments of the Czech Academy of Science, Brno, Czech Republic.*

**Corresponding author: zouharm@isibrno.cz*

Since the micro-structure or nano-structure of steels determines their mechanical properties, visual analysis of the imaged samples can provide important information about such characteristics. In order to increase efficiency of the steel industry, it is highly desirable to automate such visual analysis as much as possible. Hence we present a semi-automated Python-based tool that implements and automates the Circular Line Method (CLM) [1] for analysing distance of pearlite lamellae in steel samples. The core functionality of this application is in a rather advanced development stage.

The input images consist of two basic constituents – “dark” matrix and “light” thin pearlite lamellae, see Fig. 1 (provided by our industrial partner [2]). High contrast between the matrix and lamellae ensures that the segmentation into the individual constituents can be performed using a simple threshold and no advanced method, such as machine learning, is necessary. Then one proceeds with the CLM by counting intersections of lamellae with each of the circles from which the relevant structure factor, of known relation to mechanical properties, can be derived.

[1] LI, Zhen-Xing; etal. “Influence of Initial Pearlite Morphology on the Microstructure Evolution During Heat Treatment of 1.0C–1.5Cr Steel.” Metals and Materials International 25, 9-17 (2019); https://doi.org/10.1007/s12540-018-0171-y

[2] Třinecké Železárny, a. s./Moravia Steel a.s., Třinec, Czech Republic.

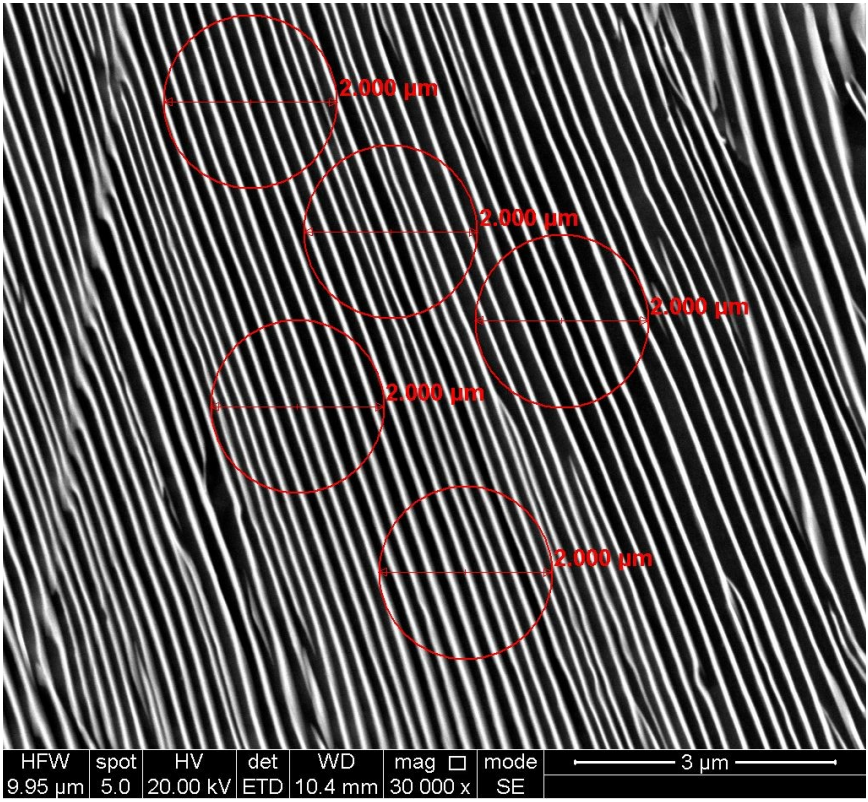

Figure 1. Example input image from manually processed test data – red overlay indicates the regions of interest used in the processing.

Fabrication of Al_2O_3 and SiC ceramics by digital light processing technology

Guifang Han*, Sijie Wei, Jian Sun, Guanghui Min

[1]*Shandong University, School of Materials Science and Engineering, Jinan, Shandong Province, China.*

**Corresponding author: gfhan@sdu.edu.cn*

Ceramics normally have high hardness, low toughness, and poor machinability, resulting in increased processing difficulties and higher costs for the manufacture of complex and precise ceramic parts. 3D printing provides a new approach to the fabrication of complex structured ceramics. However, the mechanical properties of printed ceramics are much lower than those fabricated by traditional methods. Besides, deep-colored SiC has strong light absorption and a refractive index much higher than that of resin. This seriously reduces the penetration depth of light and thereby its curing thickness. Here in this report, combined sintering additive and in-situ formation of plate-like grains were introduced to enhance the mechanical property of Al_2O_3 by digital light processing technique. A SiO_2 shell was formed by pre-oxidation of SiC powders to improve its curing ability, which was further converted into high strength mullite phase during sintering process via the design of additives. Complex shaped Al_2O_3 and SiC were successfully fabricated.

A new principle of Silicon Removal from Aluminum through Selective Extraction and Phase Separation

Hideki ONO[1*], Kenjiro MAEDA[2], Kengo KATO[1]

[1]*Academic Assembly, Faculty of Sustainable Design, University of Toyama, Toyama, Japan.*

[2]*Graduate School of Science and Engineering, University of Toyama, Toyama, Japan.*

**Corresponding author: ono@sus.u-toyama.ac.jp*

The smelting process of aluminum ore requires a large quantity of electric energy, whereas the melting and recycling of used aluminum products consumes less energy. Therefore, aluminum recycling can reduce energy consumption to not more than 1/10 of primary aluminum production. Accordingly, the recycling of aluminum is a critical issue to achieve carbon neutrality. Because Al scrap recovered from the society contains the alloying elements and the elements that are mixed in during recovery as impurities, the aluminum scraps are mainly recycled into the cast alloys which has a high tolerance level of impurities. Currently, cast Al alloy is used for engines and transmissions of automobiles. In the future, the electric car will become more popular. Thus, the demand for automobile engines and transmissions will be decreased, and scraps of the cast Al alloys may be surplus in society. Accordingly, recycling Al scrap into wrought alloy is essential. However, major components of aluminum alloy (Si, Mn, Fe, Ni, Cu, and Zn etc.) are difficult to be removed in the current pyrometallurgical processes. Therefore, a new principle to remove impurities from molten aluminum is necessary to realize the recycling process of aluminum scraps into wrought aluminum

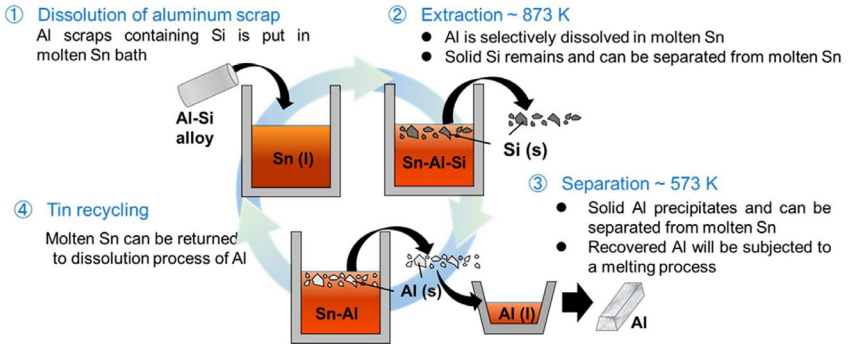

Figure 1. Concept of aluminum recycling through the selective extraction of aluminum and phase separation.

alloys. This study proposes a new principle of impurity removal from aluminum with the application of the pyrometallurgical knowledge of extraction and phase separation. Aluminum can dissolve in molten tin, whereas silicon cannot. The difference in the dissolution behavior of Al and Si into molten tin can be utilized for the selective extraction of aluminum from aluminum scraps, and aluminum can be separated from the residues consisting of silicon. The concept of aluminum recycling through the selective extraction of aluminum and phase separation is described in Fig. 1.

Aluminum scraps containing silicon are put in a tin solvent at the melting point of aluminum and aluminum can be dissolved selectively into the molten tin. Molten Sn-Al alloy can be obtained by separating the silicon from the alloy. When the molten Sn-Al alloy is cooled to the melting point of tin, aluminum with low impurity content will precipitate. In this study, Al-12mass%Si was put in Sn(l) and the new principle of Si removal was examined. Figure 2 shows the Si distribution in the sample after experiments obtained by SEM-EDS. It was found that coarse Si precipitates existed on the top of the sample and no coarse Si precipitate was observed at the bottom. The Si and Al content of the bottom part of the sample was analyzed by ICP-AES and the results showed that the Si content of Al can be lower than the initial content and the new principle of Si removal was proved effective.

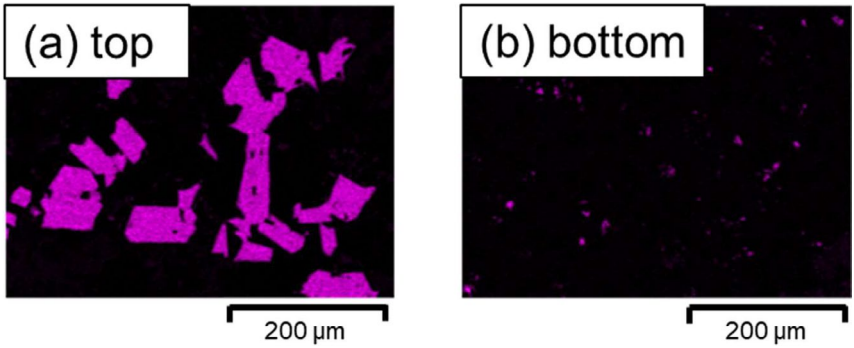

Figure 2. Si distribution in the sample after experiments (**a**) at the top, and (**b**) at the bottom.

Effect of aging precipitation behavior on corrosion resistance of Al-Mg-Zn high strength aluminum alloys

Yong Zou[1*], Fuqiang Guo[1]

[1]*School of Materials Science and Engineering, Shandong University, Jinan 250061, China*

**Corresponding author: yzou@sdu.edu.cn (Yong Zou)*

Al-Mg-Zn aluminum alloys can achieve high strength by aging because of their abundant alloying elements, but they have poorer corrosion resistance than other series of aluminum alloys. In this study, the stress corrosion behaviors of Al-Mg-Zn aluminum alloys were investigated by immersion corrosion, electrochemical and slow strain rate tension. The corrosion resistance under different heat treatment processes were compared, and the influence of the type and distribution of precipitated phases on the corrosion performance was analyzed. As a sample, the corrosion resistance of 7055 Al-Zn-Mg alloy corrosion behavior can be improved after the retrogression re-aging (RRA) treatment. After the retrogression re-aging treatment, samples showed the isolated precipitates on grain boundaries (GBs) and have a larger fraction of the low angle grain boundaries (LAGBs) than the peaking aging samples. The samples after being retrogression re-aging treatment showed better corrosion resistance than that of the single-stage peak aging samples. The results of electrochemical impedance spectroscopy (EIS) show that impedance spectrum is consisted of semi-infinite layer diffusion impedance and stagnant Weber impedance. The semi-infinite layer diffusion impedance corresponded a limited retention layer on the electrode surface. In corrosion process, Weber impedance corresponded to stagnant layer of corrosion products generated by the anode branches.

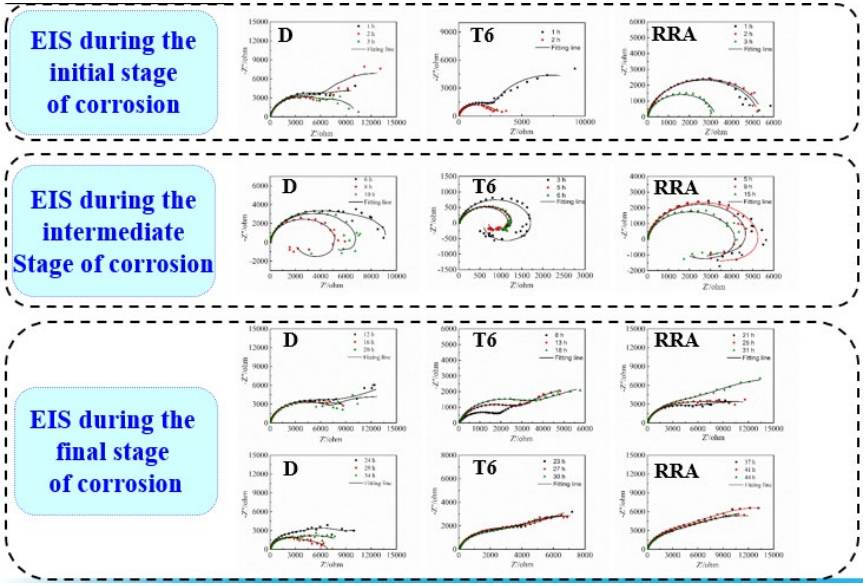

Figure 1. EIS result of 7075 aluminum alloy at different corrosion stages.

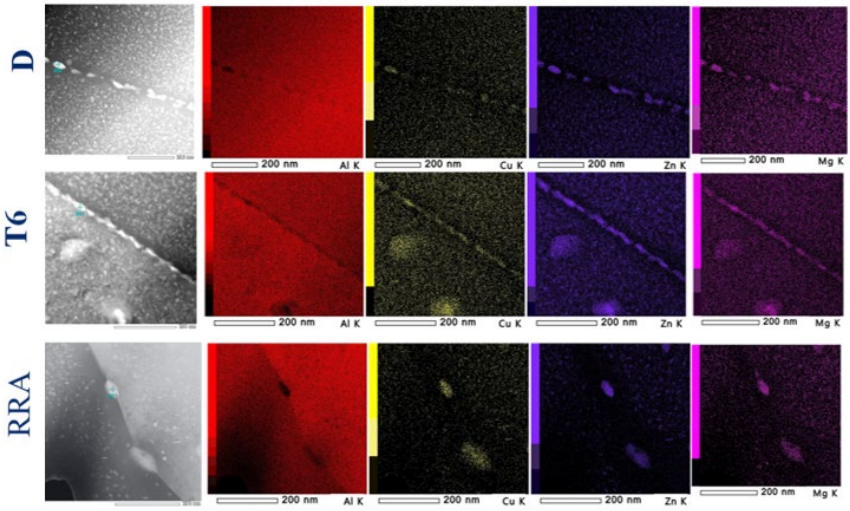

Figure 2. EDS result of the precipitated phase around the grain boundary.

Surface Modification of Recycled Aluminum Material Using a Laser

Atsushi SAIKI*, Takashi HASHIZUME

Department of Materials Design and Engineering, School of Sustainable Design, University of Toyama, Toyama, Japan

**Corresponding author: saiki@sus.u-toyama.ac.jp*

Impurity elements on the surface of aluminum alloys recycled from scrap cause problems such as stains and dirt during surface treatments such as anodizing, making them unusable for applications such as aluminum sashes, which are used without painting. In this study, a pulsed fiber laser was used. The laser output, pulse frequency, beam diameter, focus position, scan density, scanning speed, repetition rate, irradiation interval, Q value and other parameters were varied to examine the changes in microstructure and composition on the surface. If the energy to be dissipated is small relative to the energy input, transpiration will occur preferentially. For example, at the wavelength of a fiber laser (1064 nm), the absorption of Fe is about 32%, while that of Al is 8%. Also, because of the high thermal conductivity in aluminum, the irradiated laser energy is rapidly diffused into the bulk. Therefore, Fe as an impurity tends to be reduced at low power and high pulse frequency without significantly changing the surface. In addition to Fe, Si and Cu can also be reduced, and by combining irradiation conditions, multiple elements can be reduced, resulting in reduced dullness and graying after anodizing and improved color reproduction of dyes.

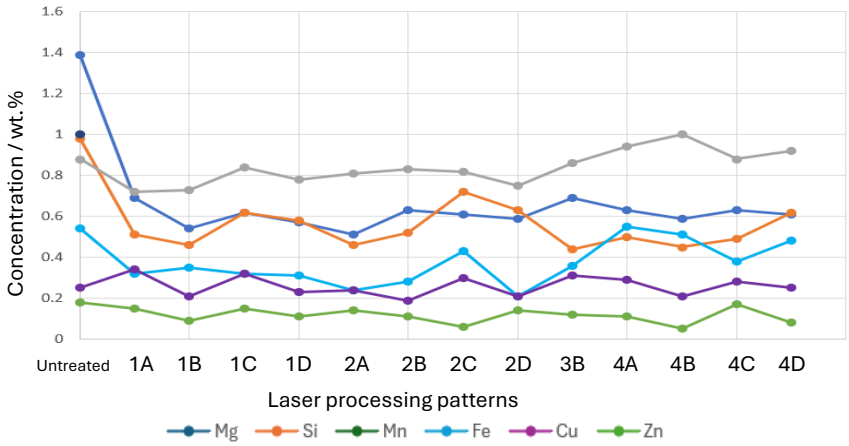

Figure 1. Change in concentration of each element after laser irradiation to the recycled aluminum.

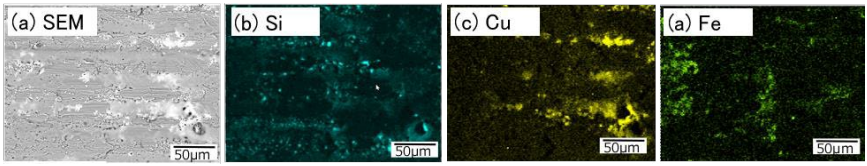

Figure 2. Surface SEM image and element distribution state of (b) Si, (c) Cu, (d) Fe after laser irradiation.

Modification of sulfur-based solid-state electrolyte films and properties of all-solid-state batteries

Lin Zhang[1*], Tao Liu[1,2], Yunfei Ma[1,2], Kangrong Lai[2], Guoqing Zhao[1], Guanghui Min[1], Lijie Ci[3]

[1]Key Laboratory for Liquid-Solid Structural Evolution & Processing of Materials (Ministry of Education), School of Materials Science and Engineering, Research Center for Carbon Nanomaterials, Shandong University, Jinan, China

[2]Department of Physics, Changji University, Changji, China

[3]State Key Laboratory of Advanced Welding and Joining, School of Materials Science and Engineering, Harbin Institute of Technology, Shenzhen, China

**Corresponding author: zhanglin2007@sdu.edu.cn*

Lithium-ion batteries play an irreplaceable role in the field of portable electronic equipment and electric vehicles because of their high energy density, high power density and long cycle life. However, the high volatility and potential fire hazard of liquid electrolyte badly limit its practical application. All-solid lithium batteries use non-flammable solid electrolytes, which can provide better energy density while avoiding the safety issues of lithium metal batteries using organic electrolytes.

Li6PS5Cl (LPSCl) is considered as one of the most promising solid electrolytes due to its excellent mechanical ductility and high ionic conductivity. Aiming at the low energy density of LPSCl solid-state electrolyte, the poor contact and stability between all-solid-state battery and positive/negative electrodes, this paper improved the electrochemical performance of all-solid-state lithium battery by thinning electrolyte thickness and interface regulation.

In this paper, two electrolyte modification methods and positive electrode modification strategies were used to improve the energy density of sulfide electrolyte, also a solvent-free solid interlayer with high interfacial energy was developed to improve the dendrite problem caused by the contact between LPSCl and lithium metal, which has important applications for the practical application of all-solid-state lithium-ion battery

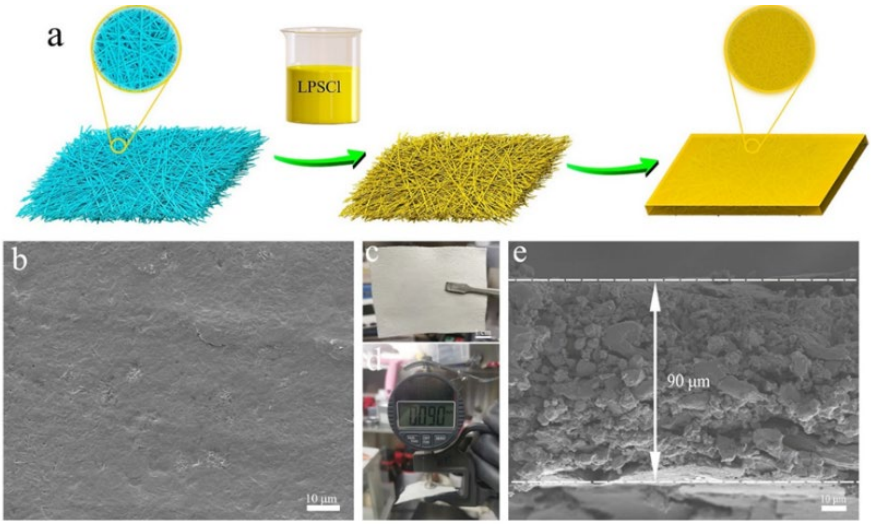

Figure 1. Morphological characteristics of the sulfide solid electrolyte film for ASSLBs. (**a**) Schematic illustration of the synthesis procedure of LPSCl film composite electrolyte for ASSLBs with slurry-casting strategy; (**b**) surface SEM image of the LPSCl film; (**c**) Optical photograph of the LPSCl film; (**d**) Cross-section optical photograph of the LPSCl film; (e) SEM image Cross-section SEM image of the LPSCl film.

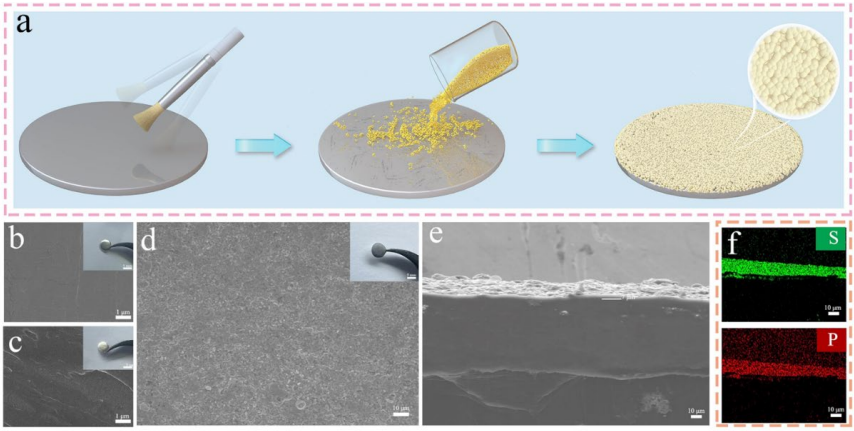

Figure 2. (**a**) Schematic illustration of the synthesis procedure of P2S5@Li for ASSLBs with solvent-free brushing method; (**b**) Li metal; (**c**) brushed Li metal; (**d**) cross-sectional morphology of P2S5@Li; (**e**, **f**) Surface morphology of P2S5@Li and the corresponding EDS mapping results.

Lithium Recovery from Spent NCM Lithium Ion Battery by Hydrogen Reduction

Jae-Ho Hwang[1], Sang-Yeop Lee[1], So-Yeong Lee[1], Ho-Sang Sohn[1*]

[1]Kyungpook National University, Department of Materials Science and Metallurgical Engineering, Daegu, Korea.

**Corresponding author: sohn@knu.ac.kr*

In this study, the effect of reduction temperature on Li recovery rates was investigated by roasting spent NCM cathode materials in a hydrogen atmosphere followed by water leaching. Weight changes were monitored while heating NCM black mass up to 1,000°C in both Ar and H2 atmospheres, with isothermal experiments conducted between 300 and 1,000°C. The reduced samples underwent water leaching, and Li concentration in the leachate was analyzed to determine recovery rates. XRD analysis was performed at each stage to study phase changes

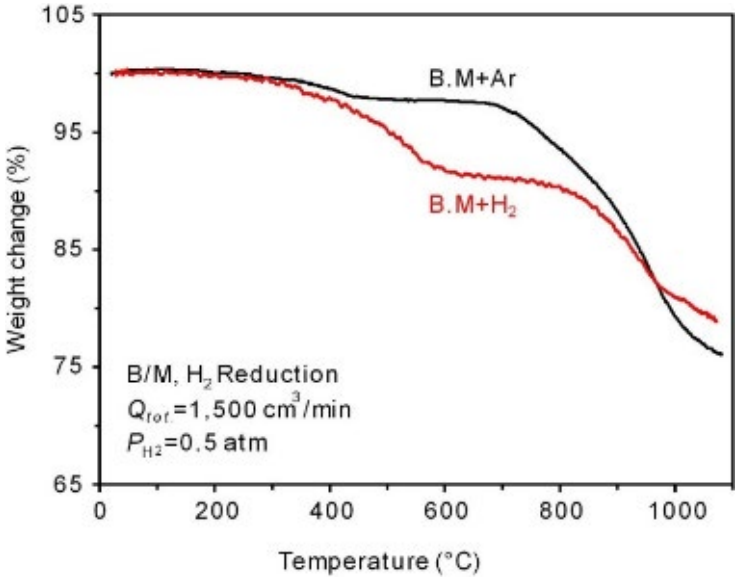

Figure 1. Thermogravimetric analysis curves of NCM in Ar gas and H_2 gas atmosphere.

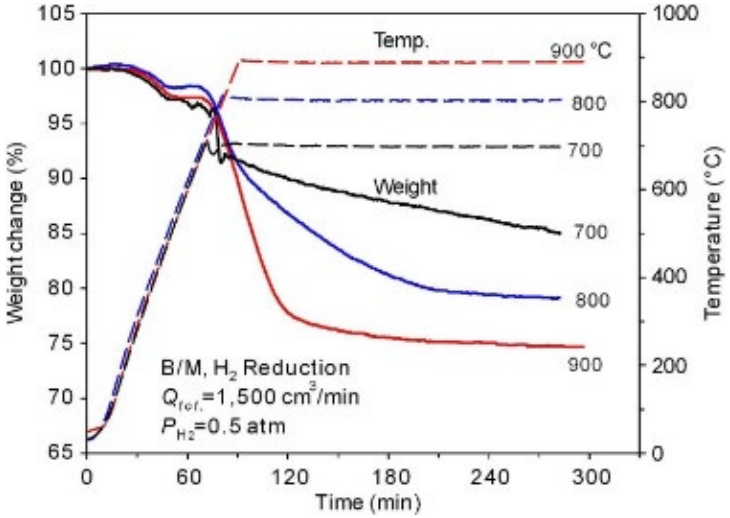

Figure 2. Themogravimetric analysis curves of isothermal experiment with different temperature in H_2 gas atmosphere.

In the Ar atmosphere, continuous weight loss was observed with increasing temperature, while in the H_2 atmosphere, weight loss began around 310°C with a secondary loss near 550°C. XRD results showed thermal decomposition of the black mass started at a lower temperature in H_2. The isothermal hydrogen reduction experiments revealed that higher temperatures led to greater weight loss rates and amounts. NiO was fully reduced to metallic Ni above 300°C, with Li_2CO_3 formation occurring above 400°C. The Li recovery rate reached approximately 90% at temperatures above 400°C.

Enhanced Anode Performance of Al-air Battery by Severe Plastic Deformation

Chaiyasit BANJONGPRASERT[1,2*], Siwat LINJEE[1], Suphitcha MOONNGAM[1,3]

[1]*Department of Physics and Materials Science, Faculty of Science, Chiang Mai University, Chiang Mai, THAILAND*

[2]*Materials Science Research Center, Faculty of Science, Chiang Mai University, Chiang Mai, THAILAND*

[3]*Office of Research Administration, Faculty of Science, Chiang Mai University, Chiang Mai, THAILAND*

**Corresponding author: chaiyasit.b@cmu.ac.th*

Aluminum-air batteries face key challenges including high self-corrosion rates and potential losses during anodic polarization. However, these issues can be mitigated through alloying and grain refinement. This research investigates the effects of grain refinement on aluminum alloys with the addition of zinc and indium (Al-Zn-In alloy) using equal channel angular pressing (ECAP), one of severe plastic deformation (SPD) technoques. The study involved analyzing the Zn/ZnO, a corrosion product of ultrafine-grained Al-Zn-In (UFG Al-Zn-In), using scanning electron microscopy, transmission electron microscopy, and X-ray diffraction. Electrochemical impedance spectroscopy (EIS), polarization curves, current-voltage curves, and anode performance tests were conducted to thoroughly examine the impact of alloying and grain refinement.

The results revealed that the UFG Al-Zn-In sample exhibited the highest energy density, voltage, and power density. The increase in grain boundaries due to ECAP, combined with the zinc and indium additions, enhanced electrochemical activity. For UFG Al-Zn-In, the electrochemical reaction occurred uniformly across the sample surface, aided by the even distribution of intermetallic compounds and the significant increase in grain boundaries. This led to uniform corrosion exclusively on the UFG Al-Zn-In. Additionally, the Zn/ZnO product on the UFG Al-Zn-In surface improved discharge stability and robustness compared to coarse-grained Al-Zn-In, resulting in a more stable discharge performance. In addition, the possibility of other flexible SPD techniques to enhance the anode performance will be discussed.

ICPMAT 2024

BRNO, 30th SEPTEMBER—3rd OCTOBER